



## Design and synthesis of Grp94 selective inhibitors based on Phe199 induced fit mechanism and their anti-inflammatory effects



Shicheng Xu <sup>a, b, 1</sup>, Anping Guo <sup>a, b, 1</sup>, Nan-nan Chen <sup>a, b</sup>, Wei Dai <sup>a, b</sup>, Huan-aoyu Yang <sup>a, b</sup>, Wenqin Xie <sup>a, b</sup>, Mengjie Wang <sup>a, b</sup>, Qi-Dong You <sup>a, b, \*\*</sup>, Xiao-Li Xu <sup>a, b, \*</sup>

<sup>a</sup> State Key Laboratory of Natural Medicines, Jiangsu Key Laboratory of Drug Design and Optimization, China Pharmaceutical University, Nanjing, 210009, China

<sup>b</sup> Department of Medicinal Chemistry, School of Pharmacy, China Pharmaceutical University, Nanjing, 210009, China

### ARTICLE INFO

#### Article history:

Received 23 March 2021

Received in revised form

17 May 2021

Accepted 1 June 2021

Available online 9 June 2021

#### Keywords:

Grp94 inhibitors

2-Amino-5-ethynylbenzamide derivatives

Ulcerative colitis

### ABSTRACT

Glucose-regulated protein 94 (Grp94), a member of the Heat shock protein 90 (Hsp90) family, is implicated in many human diseases, including cancer, neurodegeneration, inflammatory, and infectious diseases. Here, we describe our effort to design and develop a new series of Grp94 inhibitors based on Phe199 induced fit mechanism. Using an alkynyl-containing inhibitor as a starting point, we developed compound **4**, which showed potent inhibitory activity toward Grp94 in a fluorescence polarization-based assay. With improved physicochemical properties and suitable pharmacokinetic properties, compound **4** was advanced into in vivo bioactivity evaluation. In a dextran sulfate sodium (DSS)-induced mouse model of ulcerative colitis (UC), compound **4** showed anti-inflammatory property and reduced the levels of pro-inflammatory cytokines (TNF- $\alpha$  and IL-6). Together, these findings provide evidence that this approach may be promising for further Grp94 drug development efforts.

© 2021 Elsevier Masson SAS. All rights reserved.

## 1. Introduction

Heat shock protein 90 (Hsp90) is a kind of widely expressed and highly conventional molecule chaperone protein, which plays a pivotal role in the maintenance of protein homeostasis by regulating the maturation and secretion of client proteins [1,2]. The dysregulation of Hsp90 is associated with kinds of human diseases, including cancer, neurodegeneration, inflammatory and infectious diseases [3–5]. Although more than 15 N-terminal Hsp90 inhibitors have entered clinical tests for the treatment of multiple malignant tumors, none of Hsp90 inhibitors have been approved for listing through clinical trials for the lack of efficacy, toxicity, and off-target effects [6,7]. The most common adverse events are diarrhea, fatigue, nausea, and anorexia [8,9]. The main reason can be attributed

to two aspects: on the one hand, the inhibition of Hsp90 can induce the activation of heat shock transcription factor 1 (HSF1). After the activation of HSF1, Hsp 70 and Hsp 27 will be overexpressed to protect cells from apoptosis and offset the activity of Hsp90 inhibitors. On the other hand, Hsp90 is also highly expressed in normal cells. It is perceived that Hsp90 pan-inhibition might generate unaccepted toxicity and off-target effects [4,10–12]. With increasing comprehension of Hsp90 chaperone system and the modes of Hsp90-cochaperone-client complex interaction, novel regulation strategies have emerged, including inhibiting the Hsp90 C-terminal [13–16], inhibiting the interaction of Hsp90-cochaperone-client complex [17–20], and targeting the isoforms of Hsp90 (Fig. 1) [10,21–25].

Mammalian Hsp90 has four isoforms: Hsp90 $\alpha$  and Hsp90 $\beta$  in the cytosol, tumor necrosis factor receptor-associated protein-1 (Trap-1) in the mitochondria, and glucose-regulated protein 94 (Grp94) in the endoplasmic reticulum [26]. Considering that each Hsp90 isoform is responsible for chaperoning specific client proteins, selective inhibition of Hsp90 isoform might obtain better efficacy and fewer toxicities [27]. Grp94, serving as the chaperone protein of Toll-like receptors (TLRs), integrins, human epidermal growth factor receptor-2 (HER2), and Wnt coreceptor low-density lipoprotein receptor-related protein 6 (LRP6), correlates closely

\* Corresponding author. State Key Laboratory of Natural Medicines, Jiangsu Key Laboratory of Drug Design and Optimization, China Pharmaceutical University, Nanjing, 210009, China.

\*\* Corresponding author. State Key Laboratory of Natural Medicines, Jiangsu Key Laboratory of Drug Design and Optimization, China Pharmaceutical University, Nanjing, 210009, China.

E-mail addresses: [youqd@163.com](mailto:youqd@163.com) (Q.-D. You), [xuxiao\\_li@126.com](mailto:xuxiao_li@126.com) (X.-L. Xu).

<sup>1</sup> The two authors contribute equally.

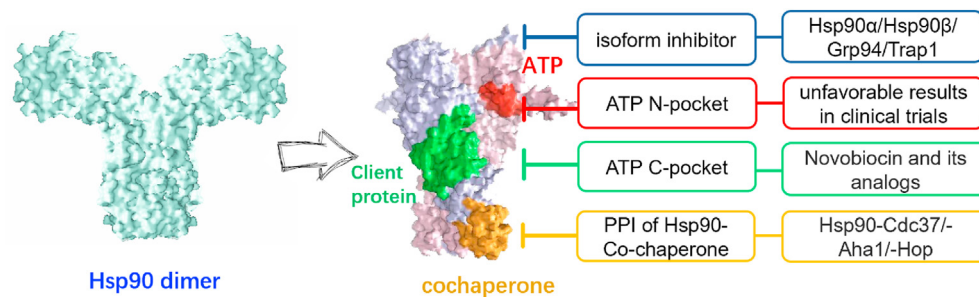


Fig. 1. Regulation strategies of Hsp90 chaperone system.

with the growth and metastasis of aberrant cancers, including breast cancer, multiple myeloma, and inflammation-associated colon cancer [28,29]. Grp94 is also involved in regulating insulin like growth factor I/II (IGF-I/II) and channeling immune and inflammatory signals [30]. As a potential therapeutic target for the diseases, Grp94-selective inhibitors have been pursued by medicinal chemists in recent years.

The homology of the N-terminal ATP binding pocket of each Hsp90 isoform is as high as 85%, which brings great difficulties to the development of selective inhibitors [31–33]. Compared with Hsp90 $\alpha/\beta$ , a 5-amino acid sequence of QEDGQ inserted at amino acid 182 in Grp94, just in the 1,4,5-helix substructure of the ATP binding pocket, causing the ATP pocket to undergo conformational changes under the induction of small ligand, thereby exposing new hydrophobic site 2 and 3 pockets next to the ATP pocket [23,34,35]. Hsp90 $\alpha/\beta$  cannot undergo conformational changes induced by small molecules, which provides a structural basis for the development of inhibitors that selectively target Grp94 [36–38].

Several Grp94 selective inhibitors that have been reported so far firstly occupy the hinge region in the Grp94 ATP pocket, and then fragments occupy the exposed specific hydrophobic pockets to achieve selectivity (Fig. 2) [36]. NECA, as an adenosine receptor agonist, was found to bind to Grp94 with a  $K_d$  value of 200 nM, becoming the first selective inhibitor of Grp94 [39,40]. The 5'-ethylcarbamoyl group of NECA can occupy the newly exposed hydrophobic site 3 near the ATP pocket. Because NECA is also a potent

adenosine receptor agonist, its further application is limited. The Gabriela Chiosis research group of the Kettering Cancer Center studied the reported Hsp90 inhibitors and found that some purine-scaffold inhibitors represented by **PU-H54** in the backward bent conformation have shown selective Grp94 inhibitory activity [23]. Through structure activity relationship (SAR) study, the compound **PU-WS13** (Grp94,  $K_d = 0.22 \mu\text{M}$ ; Hsp90 $\alpha$ ,  $K_d > 250 \mu\text{M}$ ) with better activity and higher selectivity to Grp94 was obtained. Purine inhibitors showed different binding modes when binding to Hsp90 and Grp94. When the 8-aryl group of **PU-H54** is rotated by 80° and adopts the backward bent conformation, it can induce the rearrangement of the lid region of Grp94 by displacing Phe199, then a deep and new hydrophobic pocket 2 (by Leu 104, Leu 163, Phe199, Ala 202, Phe 203, Val211, Ile 247, and Leu 249) is exposed, which is different from the site 3 pocket. The 8-aryl group can occupy this new hydrophobic pocket. However, site 2 in Hsp90 $\alpha/\beta$  is blocked by Phe 138 [23,36]. So, this class of inhibitors shows a 100-fold selectivity to Grp94 and has an excellent anti-tumor effect. Blagg's group discovered a series of selective inhibitors of Grp94 based on resorcinol fragments. The compound **Bnlm** (Grp94  $K_d = 1.14 \mu\text{M}$ ; Hsp90 $\alpha$   $K_d = 13.1 \mu\text{M}$ ) was obtained by optimizing the radicicol-geldanamycin chimera Radamide (**RDA**), which has a selectivity of 12 folds for Grp94/Hsp90 $\alpha$  [35,41]. The binding mode of **Bnlm** is different from **PU-WS13**. **KUNG29** (Grp94  $K_d = 0.2 \mu\text{M}$ ; Hsp90 $\alpha$   $K_d = 8.2 \mu\text{M}$ ) was obtained by optimization, and the selectivity was increased to 41 times [41]. **KUNG94** is a resorcinol

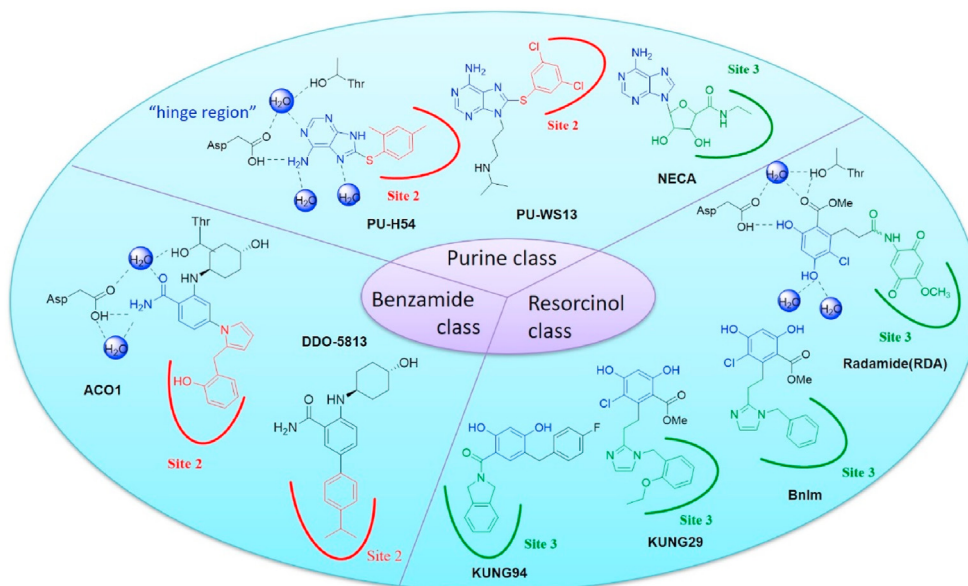


Fig. 2. Representative Grp94 inhibitors and their selective profiles.

Grp94 selective inhibitor containing an isoindoline core, with  $K_d$  of 8 nM and 77 nM for Grp94 and Hsp90 $\alpha$ , respectively [42].

Gewirth group reported that the residue Phe199, as a gate-keeper, is key to exposing site 2 in Grp94 for the design of the paralog-selective inhibitors [36]. Our group also proved that the Phe199 shift and rigid moieties in ligands are important structural bases for the design of Grp94 selective inhibitors. A new series of benzamide Grp94 selective inhibitors were developed by combining an aryl group with a benzamide scaffold [43]. Among all the Grp94 selective inhibitors, **DDO-5813** was the most potent compound with an  $IC_{50}$  value of 2 nM. However, the poor physicochemical property of compound **DDO-5813** restricts its further druggability research. Here, we report the discovery of a novel series of alkynyl-containing Grp94 inhibitors by replacing the rigid biphenyl core in **DDO-5813**. Moreover, its druggability and biological activity were also evaluated.

## 2. Results and discussion

### 2.1. Design and SAR optimization of 2-amino-5-ethynylbenzamide derivatives by in vitro Grp94 inhibitory activity

Inspired by the conclusion that ligand-induced “Phe199 shift” effect is the structural basis of Grp94-selective inhibition, a series of benzamide Grp94 selective inhibitors with biphenyl moiety were developed, among which **DDO-5813** manifested the most potent Grp94 inhibitory activity with an  $IC_{50}$  value of 2 nM [43]. However, the high fat solubility and low water solubility of compound **DDO-5813** (solubility in PBS of 3.93  $\mu$ g/mL, Log D7.4 of 4.59, permeability of  $99.18 \pm 2.61 \times 10^{-6}$  cm/s) restrict its further druggability research. The low water solubility may be related to the high crystal lattice stacking energy of biphenyl structure, which seriously affects the drug-like properties. Therefore, it is necessary to further expand the compound design around this compound in the guidance of this induced fit strategy to get more druggable molecules. In terms of spatial structure and electron cloud density, acetylene group and phenyl group are considered to be isosterisms each other in a broad sense, so replacement of the phenyl group with alkynyl groups may be useful for finding novel inhibitors with improved property. Here, we present a series of alkynyl-containing Grp94 inhibitors designed through the scaffold hopping approach by replacing the biphenyl core in **DDO-5813** with a rigid and linear alkynyl-phenyl core, which may keep the potent inhibitory potency and improve the physicochemical properties with lower crystal lattice stacking energy than biphenyl structure (Fig. 3). We performed the molecular docking studies to predict the binding modes of **DDO-5813** and compound **1** with Grp94. As for **DDO-5813**, the isopropylbenzene moiety at interposition of benzene moiety fit deeply into the hydrophobic site 2 pocket. The occupation of site 2 plays a decisive role in the improvement of inhibitory activity.

As for compound **1**, it binds to Grp94 with the critical pharmacophoric benzamide moiety and bears a rigid alkynyl substitution at interposition of benzene moiety. The alkynyl orients directly into site 2 and allows for the extension of isopropyl group to induce and occupy the site 2 pocket.

Our work started from compound **1** with an isopropyl group, which is the most potent group of biphenyl inhibitors. Compound **1** was a moderately potent inhibitor toward Grp94 ( $IC_{50} = 0.914 \pm 0.034$   $\mu$ M), which was revealed by the FP-based assays in vitro. Based on the moderate potency, we conducted further optimization on this new scaffold to develop more potent Grp94 inhibitors.

Initial SAR optimization mainly focused on the ethynyl group of **1**. In light of the fact that the isopropyl group in **1** is oriented to the induced hydrophobic pocket, substituents with different steric

effects, including *tert*-butyl, isobutyl, butyl, 1-chlorobutyl, and isopentyl, were introduced as seen in compounds **2–6**, respectively. Interestingly, significant improvements were observed in their inhibitory activities against Grp94; compound **4** with butyl-substituted showed the highest inhibitory activity ( $IC_{50} = 0.060 \pm 0.014$   $\mu$ M). We then introduced cyclopropyl, cyclopentyl, and cyclohexyl groups, affording compounds **7–9**, which maintained the inhibitory activities. We further introduced hydrophilic polar groups containing nitrogen such as N,N-dimethylaminomethyl, N,N-diethylaminomethyl as seen in compounds **10–11**, respectively. The activities significantly reduced compared with the lead compound **DDO-5813**, and the inhibitory activity towards Grp94 was almost lost. It was verified that the site 2 pocket was enormously hydrophobic and not suitable for hydrophilic polar groups. The results of SAR optimization revealed that the butyl moiety is more desirable for Grp94 inhibitory activity than rigid and bulky substituents (Table 1).

Subsequent SAR optimization mainly focused on the cyclohexanol group of **4**. Substituents with different oxygen-bearing chains, including hydroxyethyl, methoxy ethyl, ethoxy ethyl, hydroxypropyl, methoxy propyl, ethoxy propyl, and acetamino ethyl, as in **12–18**, were introduced. It was found there was a significant decrease in activity in all the cases (Table 2). The introduction of oxygen-containing five- or six-membered ring (**19–22**) seemed to be beneficial for activity, and the  $IC_{50}$  values of these compounds ranged from 0.234  $\mu$ M to 0.947  $\mu$ M, showing the six-membered ring structure is more suitable compared to five-membered ring. However, introducing a nitrogen-containing ring such as piperidyl group (**24–26**) brought about significantly decreased potency. The reduced activity may be due to the fact that they cannot form a hydrogen bond with Lys 114. So, compounds **23** and **27–34** with different acids introduced on the piperidine were designed to serve as hydrogen acceptors. However, there was no significant increase in activity. What is more, it was found that compound **26** was more potent than compound **24**. Through docking analysis, we found that compound **26** with N–H of piperidine could form hydrogen bond interaction with Glu 153.

### 2.2. Synthesis of target compounds 1-34

The synthesis of compounds **1–11** is described in Scheme 1. Different alkynes were coupled with commercial reagent **35** in THF using  $(PPh_3)_2Cl_2Pd$  and CuI as the catalysts and  $Et_3N$  as the base to afford intermediates **36–44**. The intermediates were subsequently treated with *trans*-4-aminocyclohexanol and DIPEA in DMSO at 120 °C for 16 h. The final compounds **1–9** were obtained by hydrolyzation of the cyano group into a carbamoyl group. **35** reacted with the *trans*-4-aminocyclohexanol and hydrolyzed into intermediate **45**. Then **45** was treated with various alkynes by a Sonogashira reaction to afford compounds **10–11** [43].

Compounds **12–34** were synthesized as shown in Scheme 2. Different amines reacted with the critical intermediate **39** and DIPEA in DMSO at 120 °C for 16 h followed by hydrolyzation of the cyano group to afford compounds **12–23** and intermediates **46–48**. **46–48** were reacted with silica gel in toluene at 100 °C for 48 h to afford the compounds **24–26**, respectively. Finally, **24–26** were condensed with different acids to generate desired compounds **27–31**, **32–33**, and **34**, respectively [44,45].

### 2.3. Molecular modeling

Molecular docking of compound **4** and Grp94 was conducted utilizing the software Discovery Studio (DS) 4.0 to obtain deeper insight into the mutual interactions between these alkynyl-containing compounds and Grp94. We selected the X-ray

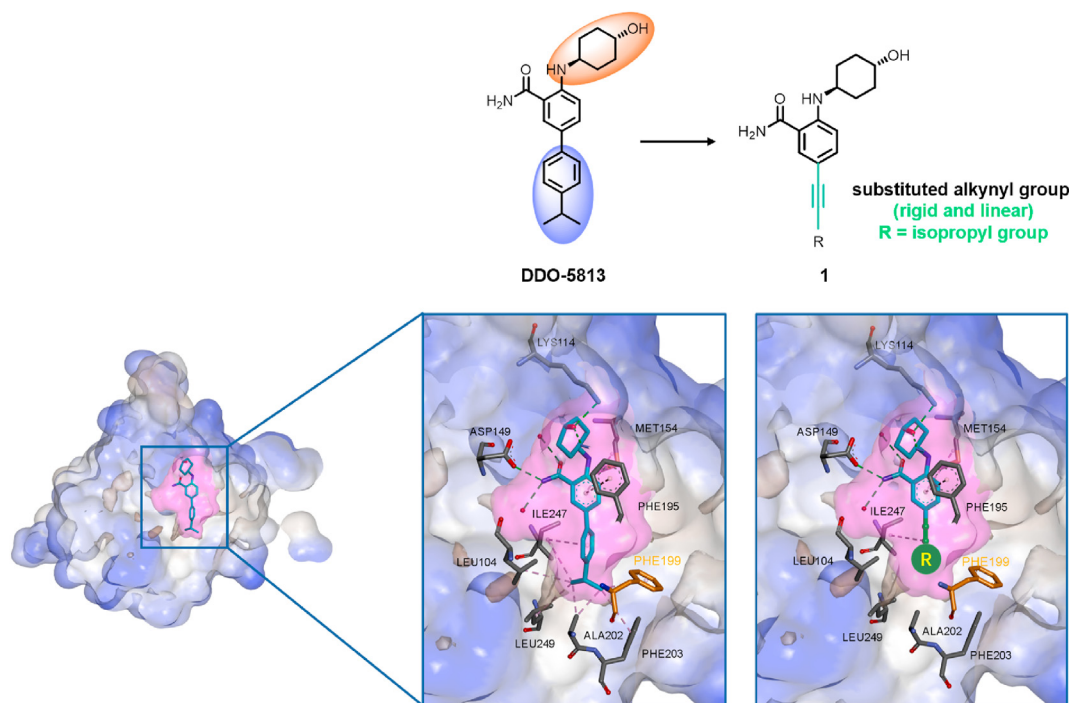


**Fig. 3.** Chemical structures of compound **DDO-5813**, the alkynyl-containing compound **1** and predicted binding poses with Grp94 (PDB ID: 3O2F). The hydrophobic surface of Grp94 is shown as blue. The active site of Grp94 is shown as purple. Compounds are shown as blue sticks. The surrounded residues are shown as grey sticks. Conserved water molecules are shown as red spheres. The H-bonds are depicted as green dashes.

crystallographic complex of Grp94 and **PU-H54** (PDB ID: 3O2F) to establish the optimized settings for docking.

The carbamoyl moiety of compound **4** formed a hydrogen bond network with Asp 149 and Thr 245, which anchored compound **4** into the ATP binding pocket. The alkynyl moiety entered into site 2 and formed interactions with the surrounding hydrophobic residues of Leu 104, Phe 195, Phe 199, Val 209, Val 211, and Ile 247. Additionally, the *trans*-4-aminocyclohexanol moiety extended to the solvent area and showed another hydrogen bond interaction with the polar residue Lys 114 (Fig. 4).

#### 2.4. Selectivity of compound **4** to Grp94 and Hsp90 $\alpha$

On the basis of the above SAR optimization, compound **4** was selected to reconfirm whether the alkynyl-containing Grp94 inhibitors represented by compound **4** selectively inhibited Grp94. BLI assay was applied to determine its potency against Grp94 and Hsp90 $\alpha$ . As shown in Fig. 5, compound **4** displayed different binding affinities for Grp94 and Hsp90 $\alpha$  ( $K_D = 0.111 \mu\text{M}$  and  $9.37 \mu\text{M}$ , respectively), which suggested that compound **4** has a remarkable Grp94 affinity and selectivity. The high Grp94 selectivity exhibited in both FP assay and BLI assay indicated that compound **4** can be a probe to study the Grp94-specific biological functions.

Moreover, different from Hsp90 $\alpha$  inhibition, Grp94-selective inhibition does not induce heat shock response and has no influence on the Hsp70 expression level. To characterize the Grp94-selective inhibitory activity of compound **4** in cells, Western blot analysis was conducted to evaluate the expression levels of the selected biomarkers in compound **4** treated HCT116 cells. As shown in Fig. 3 (see supplementary data), no modulation of Hsp70 and Akt (Hsp90 $\alpha$  specific client) was observed. In contrast, the pan-Hsp90 inhibitor AT13387 obviously induced upregulation of Hsp70 and degradation of Akt. These results confirmed that the Grp94-

selective inhibitor, compound **4**, can't activate HSF-1 and induce the up-regulation of other heat shock proteins in cells, which may reduce the side-effects of pan-isoform Hsp90 inhibition.

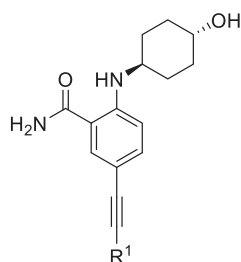
#### 2.5. Evaluation of physicochemical properties of representative compounds

The physicochemical properties of compounds have essential effects on their absorption, distribution, metabolism, and excretion in vivo. The synthesis of this series of alkynyl-containing compounds is to improve the physicochemical properties of biphenyl inhibitors. So, the partition coefficient (log  $D$ , pH 7.4), solubility, and permeability coefficients ( $P_e$ ) of representative compounds were determined. As shown in Table 3, compared with **DDO-5813**, compounds **4** and **23** have similar membrane permeability and can penetrate artificial membranes better. The water solubility of **4** and **23** is improved by 3–4 times, and log  $D_{7.4}$  is between 3–4, which gets a litter lower. Therefore, the results suggest that the structural optimization has improved the physical and chemical properties of the biphenyl compounds. Although the water solubility of **23** is slightly better than that of **4**, its inhibitory activity on Grp94 is reduced by 3 times. Considering the improved physicochemical properties and activity, we selected compound **4** for further pharmacokinetic and pharmacodynamic research.

#### 2.6. Evaluation of pharmacokinetic profiles and liver microsome stability of compound **4**

As shown in Table 4, acceptable  $T_{1/2}$  (4.69 h) was observed in rats with intragastrical administration. Compound **4** exhibited suitable bioavailability in rats (15.73%), which verified that compound **4** was worthy of further studies on efficacy in vivo. Besides, we further assessed the liver microsome stability of compound **4** in human and mouse liver microsomes in vitro, compared with

**Table 1**  
Inhibitory activity of compounds **1-11** against Grp94.



Compd.	Structure R <sup>1</sup> =	Grp94 FP activity <sup>a</sup>	
		Inhibition percentage (100 μM)	IC <sub>50</sub> (μM)
<b>1</b>		100 %	0.914 ± 0.034
<b>2</b>		100 %	0.325 ± 0.019
<b>3</b>		100 %	0.313 ± 0.021
<b>4</b>		100 %	0.060 ± 0.014
<b>5</b>		100 %	0.205 ± 0.007
<b>6</b>		100 %	0.519 ± 0.042
<b>7</b>		100 %	0.251 ± 0.017
<b>8</b>		100 %	0.100 ± 0.004
<b>9</b>		100 %	0.210 ± 0.008
<b>10</b>		63.9 %	62.627 ± 9.028
<b>11</b>		28.0 %	> 100
<b>DDO-5813</b>		100 %	0.020 ± 0.004
<b>AT13387</b>		100 %	0.013 ± 0.004

<sup>a</sup> IC<sub>50</sub> values are the mean ± SD from three independent experiments. Compound **DDO-5813** and **AT13387** were selected as positive controls. Almost all compounds exhibited 100% inhibition of Hsp90α at 100 μM (data not shown).

compound **DDO-5813**. As shown in [Table 5](#), compound **4** exhibited preferable metabolic stability in human and mouse liver microsomes ( $t_{1/2}$  = 346.5 min and 108.3 min, respectively), compared with that of **DDO-5813** ( $t_{1/2}$  = 256.7 min and 62.4 min, respectively). Meanwhile, the clearance rates of compound **4** were lower. Thus, compound **4** exhibited good stability and deserved further evaluation.

## 2.7. Evaluation of anti-inflammatory efficacy of compound **4** in a DSS-Induced UC model

Ulcerative colitis (UC) is a typical bowel disease, the morbidity of which has been increasing in recent years. Human UC symptoms include the loss of weight, severe diarrhea, the bleeding of rectal, the damage of intestinal mucosal, and the elevation of pro-inflammatory cytokines in colonic tissues [46]. The multifaceted roles of Grp94 in the development of UC have been reported in various papers. Zihai Li's group reported that Grp94 played an essential role in gut homeostasis via regulating the canonical Wnt pathway [47]. Grp94 is important for CD11c<sup>+</sup> cells in the

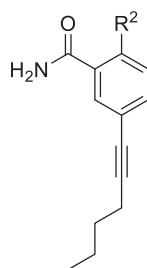
maintenance of gut homeostasis and the induction of regulatory T cells [48]. It has been reported that macrophage-specific Grp94 KO mice were more resistant to DSS-induced colitis, which indicated that Grp94 has detrimental roles in the exacerbation of intestinal inflammation [49]. However, the function of Grp94 in gastrointestinal homeostasis is not well understood, and there is an urgent need for Grp94-specific modulators to explore whether inhibition of Grp94 has some efficacy. Considering both the suitable pharmacokinetic characteristics and potent inhibitory activity of compound **4**, the efficacy of **4** was further investigated in a mouse UC model induced by DSS.

C57BL/6 mice were divided into the disease control group, treatment groups, and the normal control group. The mice in disease control group and treatment groups were given 3% DSS drinking water from day 1 to day 7. We established the UC model successfully after the observation of typical symptoms, such as weight loss, diarrhea, and rectal bleeding. Meanwhile, the treatment groups were given compound **4** with 10 mg/kg, 30 mg/kg, and 50 mg/kg by intraperitoneal injection.

As shown in [Fig. 6A](#), the body weights of all experimental mice changed slightly in the first four days. After day 4, the body weights of normal group mice increased continuously. Conversely, the weight loss was evident in the disease control group. Compound **4** could alleviate the weight loss of the mice in three treatment groups. Based on the fact that inflammation often results in enlargement of the spleen, we also investigated the changes in spleen weight index. Mice in treatment groups presented a significant decrease of spleen weight index compared to that in the disease control group, which indicated that compound **4** could ameliorate the inflammation. The liver weight index of mice in treatment groups was not significantly reduced, confirming that compound **4** was safe enough to be a potential UC treatment agent ([Fig. 6B](#)). Scoring changes in weight loss, stool consistency, and stool blood were calculated and averaged to afford disease activity index (DAI) scores. As shown in [Fig. 6C](#), compound **4** significantly decreased DAI scores in a dose-dependent manner on day 8. On day 8, mice from the disease control group showed hair brightness loss, ataxia, leanness, and severe rectal bleeding ([Fig. 6D](#)). The mice in treatment groups showed varying degrees of improvements in their appearances in the following order: 50 mg/kg, 30 mg/kg, 10 mg/kg.

Colon shortening is another symptom, which is often used to evaluate the colitis induced by DSS. However, compound **4** could not significantly prevent colon shortening induced by DSS ([Fig. 7A](#)). Similarly, administration of compound **4** could not obviously attenuate the severe colonic tissue damage induced by DSS ([Fig. 7B](#)). The reason may be that the damage induced by DSS was so substantial that compound **4** could not repair the damage within a short time. Pro-inflammatory cytokines, such as tumor necrosis factor-α (TNF-α) and interleukin-6 (IL-6), play essential roles in the pathogenesis of UC and have been implicated as important mediators of the inflammatory reaction in UC patients. To better understand the anti-inflammatory mechanism of compound **4**, enzyme-linked immunosorbent assay (ELISA) and immunohistochemical assay (IHC) were conducted to determine the levels of TNF-α and IL-6. The obvious elevation of TNF-α and IL-6 in colonic tissues was observed in DSS-treated mice by the immunohistochemical assay. Compound **4** could significantly and dose-dependently reduce the levels of TNF-α and IL-6 ([Fig. 7C](#)). We also observed compound **4** could reduce the levels of TNF-α and IL-6 in ELISA ([Fig. 7D](#)). Thus, these results demonstrated that compound **4** potentially possesses promising anti-inflammatory effects by inhibiting the pro-inflammatory cytokines, including TNF-α and IL-6.

**Table 2**  
Inhibitory activity of compounds **12-34** against Grp94.

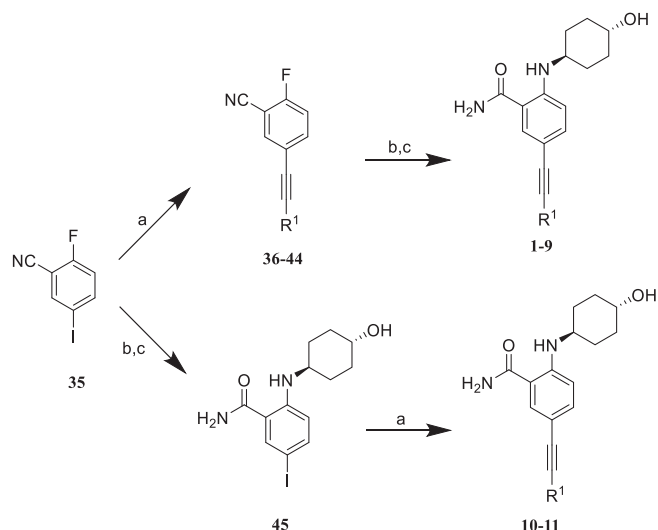


Compd.	Structure R <sup>2</sup> =	Grp94 FP activity <sup>a</sup>	
		Inhibition percentage (100 μM)	IC <sub>50</sub> (μM)
<b>12</b>		97.2 %	6.839 ± 0.323
<b>13</b>		98.9 %	10.898 ± 1.969
<b>14</b>		100 %	7.544 ± 0.481
<b>15</b>		100 %	2.769 ± 0.455
<b>16</b>		100 %	2.061 ± 0.234
<b>17</b>		100 %	3.312 ± 0.169
<b>18</b>		100 %	2.017 ± 0.336
<b>19</b>		100 %	0.310 ± 0.081
<b>20</b>		100 %	0.947 ± 0.080
<b>21</b>		100 %	0.234 ± 0.030
<b>22</b>		100 %	0.393 ± 0.065
<b>23</b>		100 %	0.203 ± 0.026
<b>24</b>		100 %	1.607 ± 0.243
<b>25</b>		65.2 %	16.599 ± 1.141
<b>26</b>		100 %	0.627 ± 0.007
<b>27</b>		100 %	0.528 ± 0.024
<b>28</b>		100 %	0.797 ± 0.060
<b>29</b>		97.8 %	1.108 ± 0.122

Table 2 (continued)

Compd.	Structure R <sup>2</sup> =	Grp94 FP activity <sup>a</sup>	
		Inhibition percentage (100 μM)	IC <sub>50</sub> (μM)
30		100 %	1.488 ± 0.281
31		100 %	0.985 ± 0.044
32		90.2 %	4.779 ± 0.330
33		94.3 %	2.405 ± 0.264
34		98.6 %	2.045 ± 0.269

<sup>a</sup> IC<sub>50</sub> values are the mean ± SD from three independent experiments. Almost all compounds exhibited 100% inhibition of Hsp90α at 100 μM (data not shown).



**Scheme 1.** Synthetic routes for compounds 1–11. Reagents and conditions: (a) different alkynes, CuI, (PPh<sub>3</sub>)<sub>2</sub>Cl<sub>2</sub>Pd, Et<sub>3</sub>N, rt, 8 h; (b) *trans*-4-aminocyclohexanol, DIPEA, DMSO, 120 °C, 16 h; (c) 2 M NaOH, 30% H<sub>2</sub>O<sub>2</sub>, EtOH, DMSO, 30 °C, 12 h.

### 3. Conclusion

In this study, computational methods and medicinal chemistry were used to design and synthesize more potent Grp94 inhibitors. Based on the conclusion that the ligand induced “Phe199 shift” effect contributes to the selective inhibition of Grp94, a novel series of alkynyl-containing Grp94 inhibitors were developed by replacing the phenyl ring at interposition of benzene moiety with rigid and linear alkynyl substituents. Compound **4** with highest inhibitory activity *in vitro*, preferable stability, and improved physical properties was used for further investigations. In light of the excellent PK properties *in vivo*, compound **4** was selected further to confirm the anti-inflammatory effects in the DSS-challenged mouse model. The results showed that compound **4** could reduce the levels of circulating pro-inflammatory cytokines (TNF-α and IL-6) in colonic tissues and improve the inflammatory responses of UC mice. The loss of body weights in treatment group mice was

alleviated by compound **4**, and the DAI scores in the treatment group mice were obviously lower than those in the disease control group mice. These results revealed that compound **4** is an orally active anti-inflammatory agent for the treatment of UC.

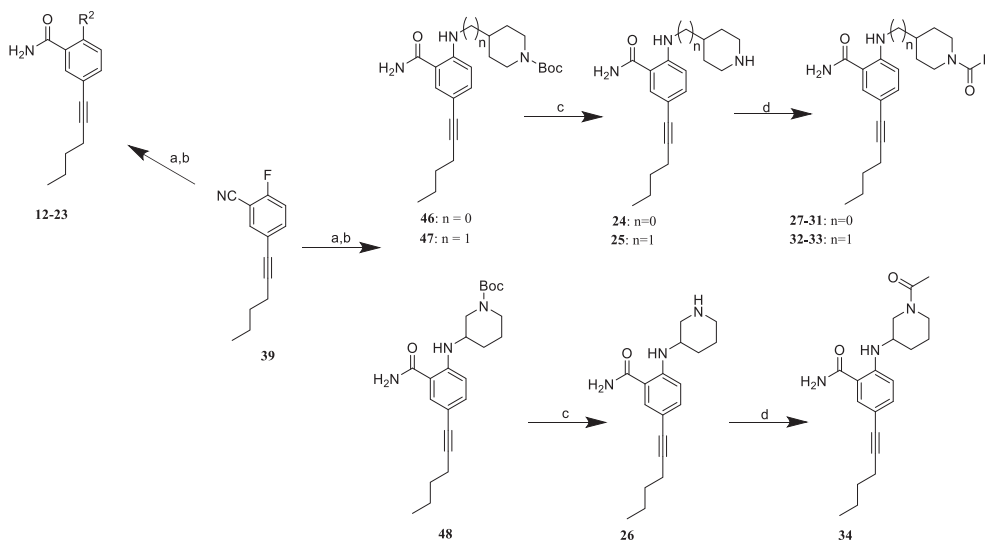
### 4. Experimental section

#### 4.1. General methods and materials

All reagents and solvents purchased from commercial suppliers were used directly. Thin-layer chromatography (TLC) was carried out on 0.25 mm silica gel plates (GF254) to monitor reactions, and spots were visualized with UV light. Melting points were determined with a Melt-Temp II apparatus. The structures of synthesized compounds were characterized by <sup>1</sup>H NMR, <sup>13</sup>C NMR, MS, and HRMS. The <sup>1</sup>H NMR and <sup>13</sup>C NMR spectra were measured on a Bruker AV-300 instrument using deuterated solvents with tetramethylsilane (TMS) as an internal standard. ESI-mass and high-resolution mass spectra (HRMS) were recorded on a Water Q-ToF micro mass spectrometer by electrospray ionization (ESI). The purity (≥95%) of the compounds was verified by the high-performance liquid chromatography (HPLC) performed on an Agilent C18 (4.6 mm × 150 mm, 3.5 μm) column using a mixture of solvent methanol/water at a flow rate of 0.5 mL/min and monitored by UV absorption at 254 nm. The LC/MS analyses were carried out on HPLC-MS system with a triple quadrupole mass spectrometer (Shimadzu) using an Inertsil C18 column at a flow rate of 0.4 mL/min.

#### 4.2. Synthesis

**4.2.1. General Procedure for intermediates 36–44.** (PPh<sub>3</sub>)<sub>2</sub>Cl<sub>2</sub>Pd (0.01 equiv), CuI (0.02 equiv), and Et<sub>3</sub>N (5.0 equiv) were added to a mixture of **35** (1.0 equiv) and appropriate alkyne (2.0 equiv) in THF and stirred at room temperature for 8 h under nitrogen protection. After confirming the progress of the reaction by thin-layer chromatography, the black reaction mixture was filtered, and the filtrate was concentrated under vacuum. EA (20 mL) was added, and the organic layer was washed with water and brine, dried over anhydrous sodium sulfate, and concentrated *in vacuo*. Purification by silica gel chromatography (petroleum ether) afforded



**Scheme 2.** Synthetic route for compounds **12–34**. Reagents and conditions: (a) different amines, DIPEA, DMSO, 120 °C, 16 h; (b) 2 M NaOH, 30% H<sub>2</sub>O<sub>2</sub>, EtOH, DMSO, 30 °C, 12 h; (c) silica gel, toluene, 100 °C, 48 h; (d) different acids, BOP, DIPEA, DMF, rt, 4 h.

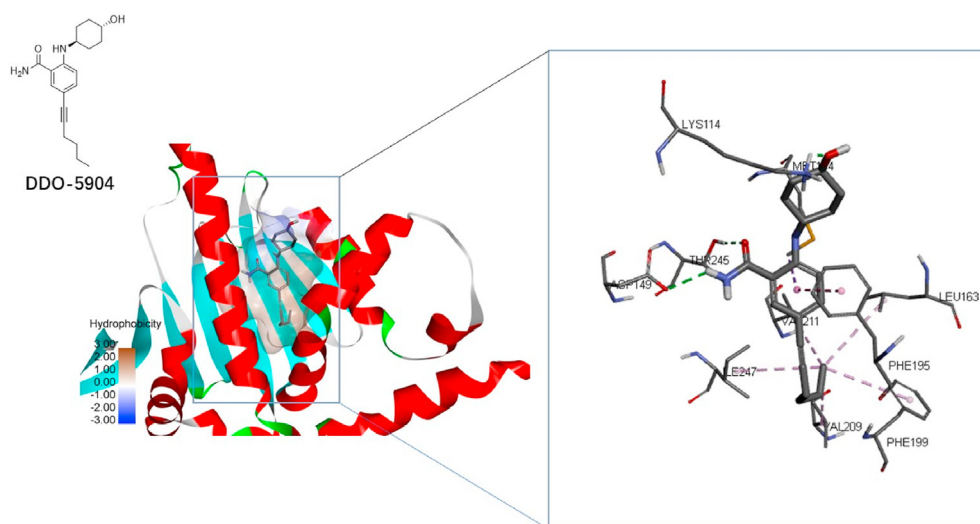


**Fig. 4.** Docking study of the binding mode between **4** and Grp94 (PDB ID: 3O2F). The surface of Grp94 is shown in the hydrophobic state. The carbon atoms of the ligands and Grp94 residues are colored grey. The hydrogen bonds are represented as green dashed lines.

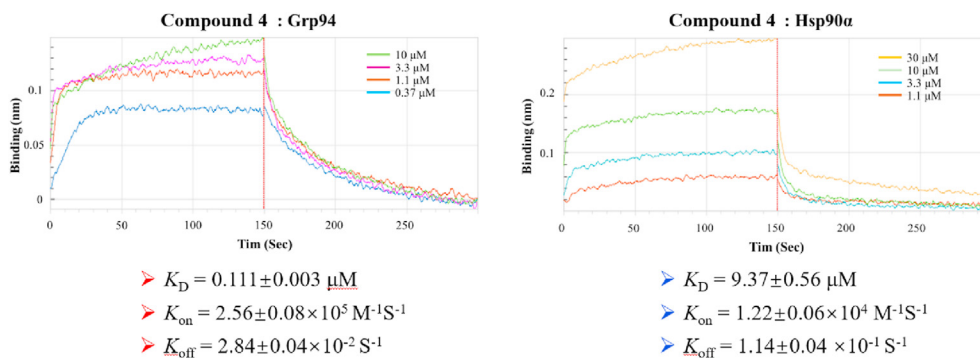


**Fig. 5.** BLI dose–response curves of **4** binding to Grp94 and Hsp90α.

**Table 3**  
Physicochemical properties of the compounds **4**, **23**, and **DDO-5813**.

Compd.	Physicochemical properties		
	Log D pH = 7.4	Solubility ( $\mu\text{g/mL}$ )	Pe, pH 7.4 <sup>a</sup> ( $10^{-6}$ cm/s)
<b>4</b>	3.69	11	97.86 $\pm$ 1.50
<b>23</b>	3.24	16	94.61 $\pm$ 0.22
<b>DDO-5813</b>	4.59	3.9	99.18 $\pm$ 2.61

<sup>a</sup> Data are presented as mean  $\pm$  SD of three separate experiments.**Table 4**  
Pharmacokinetic profiles of compound **4**.

PK parameters	<b>4</b>	
	rat (iv, 10 mg/kg)	rat (po, 40 mg/kg)
T <sub>max</sub> (h)	0.05	0.38
T <sub>1/2</sub> (h)	15.25	4.69
C <sub>max</sub> ( $\mu\text{g/mL}$ )	2.41	0.60
AUC <sub>0-∞</sub> (h· $\mu\text{g/mL}$ )	1.51	0.95
V <sub>z</sub> (L/kg)	1.47	2.81
CL (L/h/kg)	6.66	4.37
F (%)		15.73

**Table 5**  
In vitro metabolic stability of compound **4** and **DDO-5813** in human and mouse liver microsomes.

Compd	human liver microsomes		mouse liver microsomes	
	T <sub>1/2</sub> (min)	CL ( $\mu\text{L/min/mg}$ )	T <sub>1/2</sub> (min)	CL ( $\mu\text{L/min/mg}$ )
<b>4</b>	346.5	11.0	108.3	12.8
<b>DDO-5813</b>	256.7	13.5	62.4	25.5

intermediates **36–44**.

4.2.1.1. 2-fluoro-5-(3-methylbut-1-yn-1-yl)benzotrile (36). Intermediate **36** was prepared from **35** (370 mg, 1.5 mmol) and 3-methylbut-1-yne (204 mg, 3.0 mmol) according to the general

procedures. Colorless oil (260 mg, 92.7%). <sup>1</sup>H NMR (300 MHz, chloroform-d)  $\delta$  7.66–7.53 (m, 2H), 7.14 (t,  $J$  = 8.7 Hz, 1H), 2.82–2.72 (m, 1H), 1.26 (d,  $J$  = 6.9 Hz, 6H).

4.2.1.2. 2-fluoro-5-(3,3-dimethylbut-1-yn-1-yl)benzotrile (37). Intermediate **37** was prepared from **35** (370 mg, 1.5 mmol) and 3,3-dimethylbut-1-yne (246 mg, 3.0 mmol) according to the general procedures. White solid (295 mg, 97.8%). <sup>1</sup>H NMR (300 MHz, chloroform-d)  $\delta$  7.68–7.57 (m, 2H), 7.15 (t,  $J$  = 8.7 Hz, 1H), 1.32 (s, 9H).

4.2.1.3. 2-fluoro-5-(4-methylpent-1-yn-1-yl)benzotrile (38). Intermediate **38** was prepared from **35** (370 mg, 1.5 mmol) and 4-methylpent-1-yne (246 mg, 3.0 mmol) according to the general procedures. Light yellow oil (272 mg, 90.2%). <sup>1</sup>H NMR (300 MHz, chloroform-d)  $\delta$  7.66–7.58 (m, 2H), 7.15 (t,  $J$  = 8.6 Hz, 1H), 2.30 (d,  $J$  = 6.6 Hz, 2H), 1.98–1.85 (m, 1H), 1.04 (d,  $J$  = 6.7 Hz, 6H).

4.2.1.4. 2-fluoro-5-(hex-1-yn-1-yl)benzotrile (39). Intermediate **39** was prepared from **35** (370 mg, 1.5 mmol) and hex-1-yne (246 mg, 3.0 mmol) according to the general procedures. Colorless oil (270 mg, 89.5%). <sup>1</sup>H NMR (300 MHz, chloroform-d)  $\delta$  7.66–7.56 (m, 2H), 7.15 (t,  $J$  = 8.6 Hz, 1H), 2.41 (t,  $J$  = 6.9 Hz, 2H), 1.65–1.55 (m, 2H), 1.53–1.43 (m, 2H), 0.97 (t,  $J$  = 7.3 Hz, 3H).

4.2.1.5. 2-fluoro-5-(5-chloropent-1-yn-1-yl)benzotrile (40). Intermediate **40** was prepared from **35** (370 mg, 1.5 mmol) and 5-chloropent-1-yne (306 mg, 3.0 mmol) according to the general procedures. Light yellow oil (258 mg, 77.8%). <sup>1</sup>H NMR (300 MHz, chloroform-d)  $\delta$  7.67–7.59 (m, 2H), 7.17 (t,  $J$  = 8.6 Hz, 1H), 3.71 (t,  $J$  = 6.3 Hz, 2H), 2.63 (t,  $J$  = 6.9 Hz, 2H), 2.12–2.03 (m, 2H).

4.2.1.6. 2-fluoro-5-(5-methylhex-1-yn-1-yl)benzotrile (41). Intermediate **41** was prepared from **35** (370 mg, 1.5 mmol) and 5-methylhex-1-yne (288 mg, 3.0 mmol) according to the general procedures. Light yellow oil (288 mg, 89.3%). <sup>1</sup>H NMR (300 MHz, chloroform-d)  $\delta$  7.66–7.56 (m, 2H), 7.15 (t,  $J$  = 8.7 Hz, 1H), 2.41 (t,  $J$  = 7.4 Hz, 2H), 1.79–1.68 (m, 1H), 1.51 (q,  $J$  = 7.3 Hz, 2H), 0.95 (d,  $J$  = 6.6 Hz, 6H).

4.2.1.7. 2-fluoro-5-(cyclopropylethynyl)benzotrile (42). Intermediate **42** was prepared from **35** (370 mg, 1.5 mmol) and ethynylcyclopropane (198 mg, 3.0 mmol) according to the general

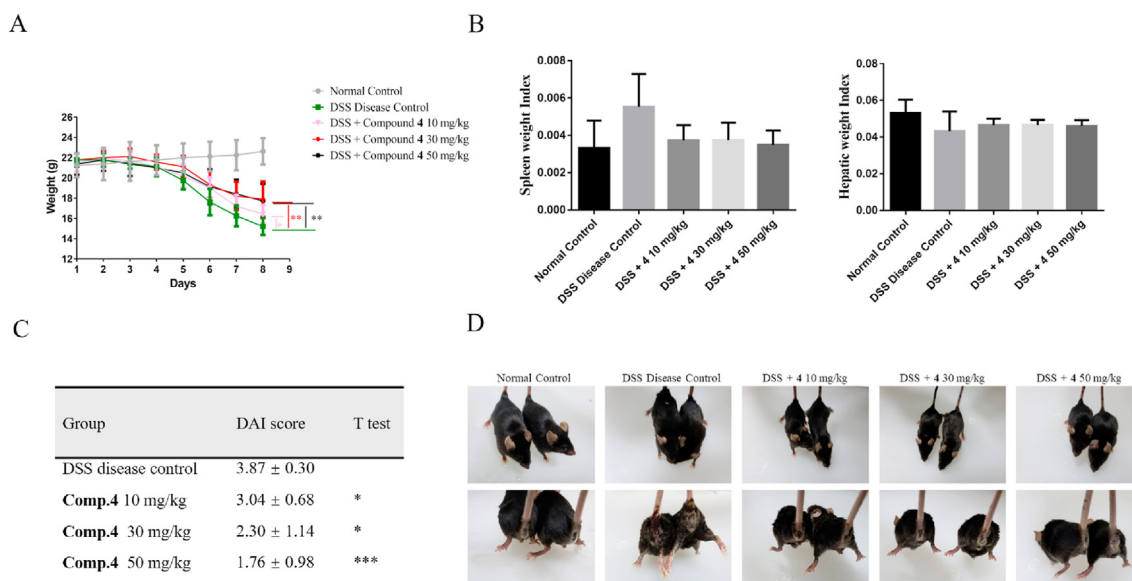


**Fig. 6.** Anti-inflammatory efficacy of compound **4** in DSS-induced UC mice. (A) Body weight changes of each group during treatment. (B) The spleen/liver weight index of each group. The spleen/liver weight index was calculated according to the following formula: spleen/liver index (mg/g) = spleen/liver weight (mg)/animal body weight (g). (C) DAI scores during treatment. Data are expressed as mean  $\pm$  SEM. The detailed scoring criteria for DAI was as follows: body weight loss (<1% = 0; 1–5% = 1; 5–10% = 2; 10–15% = 3 and > 15% = 4), stool consistency (normal = 0; slightly soft = 1; soft = 2; very soft = 3; diarrhea = 4), and stool blood (none = 0; occult blood = 2; fecal blood = 4). (D) The general status of the UC mice at day 8. Compared with the disease control group: \* $P$  < 0.05, \*\* $P$  < 0.01, \*\*\* $P$  < 0.001.

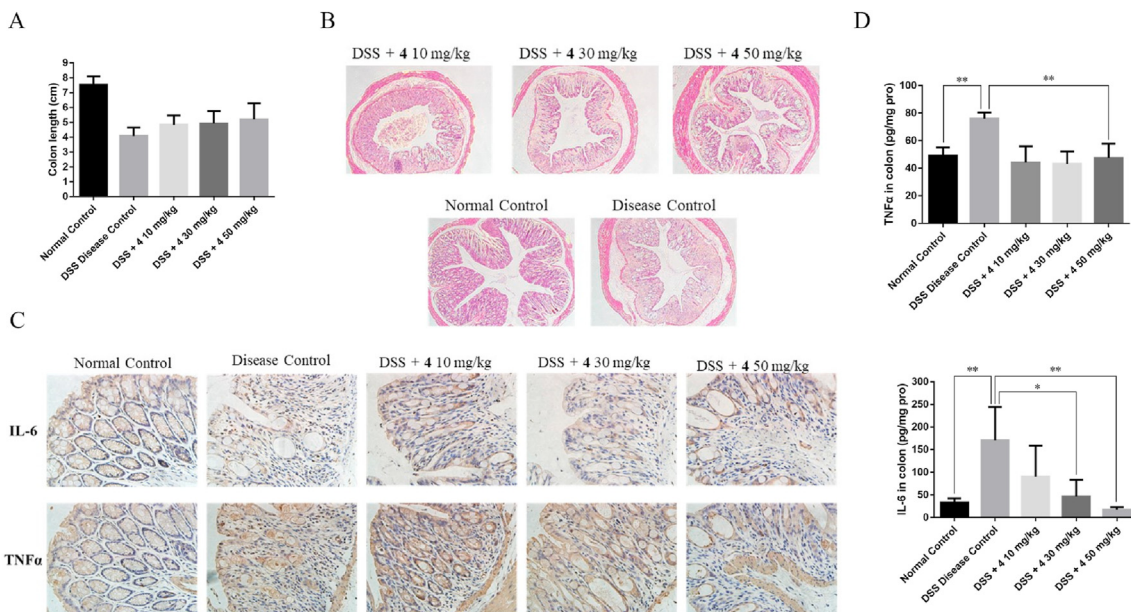


**Fig. 7.** Efficacy of compound **4** on colons from each group and the inhibitory effect of compound **4** on the up-regulated inflammatory cytokines in the colon tissues of DSS-induced UC mice. (A) Colon length of each group on day 8. (B) Representative H&E images of the colon samples from each group. Scale bar, 200  $\mu$ m. (C) The levels of TNF- $\alpha$  and IL-6 were detected in IHC. (D) The levels of TNF- $\alpha$  and IL-6 were detected in ELISA. Compared with the disease control group: \* $P < 0.05$ , \*\* $P < 0.01$ , \*\*\* $P < 0.001$ .

procedures. Light yellow oil (270 mg, 97.3%).  $^1\text{H}$  NMR (300 MHz, chloroform- $d$ )  $\delta$  7.65–7.51 (m, 2H), 7.13 (t,  $J = 8.7$  Hz, 1H), 1.49–1.40 (m, 1H), 0.96–0.86 (m, 2H), 0.85–0.79 (m, 2H).

4.2.1.8. 2-fluoro-5-(cyclopentylethynyl)benzotrile (43). Intermediate **43** was prepared from **35** (370 mg, 1.5 mmol) and ethynylcyclopentane (282 mg, 3.0 mmol) according to the general procedures. Colorless oil (266 mg, 83.2%).  $^1\text{H}$  NMR (300 MHz, chloroform- $d$ )  $\delta$  7.66–7.56 (m, 2H), 7.14 (t,  $J = 8.7$  Hz, 1H), 2.87–2.77 (m, 1H), 2.06–1.95 (m, 2H), 1.80–1.53 (m, 6H).

4.2.1.9. 2-fluoro-5-(cyclohexylethynyl)benzotrile (44). Intermediate **44** was prepared from **35** (370 mg, 1.5 mmol) and ethynylcyclohexane (324 mg, 3.0 mmol) according to the general procedures. Light yellow oil (322 mg, 94.5%).  $^1\text{H}$  NMR (300 MHz, chloroform- $d$ )  $\delta$  7.66–7.58 (m, 2H), 7.15 (t,  $J = 8.7$  Hz, 1H), 2.63–2.54 (m, 1H), 1.94–1.83 (m, 2H), 1.79–1.70 (m, 2H), 1.57–1.48 (m, 2H), 1.44–1.25 (m, 4H).

4.2.2. General Procedure for the Preparation of Compounds 1–9. To a stirred solution of the appropriate intermediate **36–44** (1.0 equiv) in DMSO were added *trans*-4-aminocyclohexanol (4.5 equiv) and DIPEA (9.0 equiv). The reaction mixture was refluxed at 120  $^{\circ}\text{C}$  for 16 h. After the reaction was finished, the reaction mixture was diluted with water, and the aqueous layer was extracted with EA. The combined EA layers were dried over anhydrous  $\text{Na}_2\text{SO}_4$ , concentrated under reduced pressure and dissolved in EtOH (15 ml) and DMSO (1 ml). The reaction mixture which was added NaOH (2 M, 2 ml), and 30%  $\text{H}_2\text{O}_2$  (2 ml) stirred at 30  $^{\circ}\text{C}$  for 12 h. After removing the EtOH by concentration under reduced pressure, the residue was dissolved in EA (20 ml), washed with water (20 ml  $\times$  2) and brine (30 mL  $\times$  3), dried over anhydrous  $\text{Na}_2\text{SO}_4$ , and concentrated in vacuo. The residue was purified by silica gel column chromatography (PE/EA, 2:1) to afford **1–9**.

4.2.2.1. 2-(((1R,4R)-4-hydroxycyclohexyl)amino)-5-(3-methylbut-1-yn-1-yl)benzamide (1). Compound **1** was prepared from intermediate **36** (260 mg, 1.39 mmol) according to the general procedures. White solid (160 mg, 38.3%). Mp 198.6–200.0  $^{\circ}\text{C}$ .  $^1\text{H}$  NMR (300 MHz, DMSO- $d_6$ )  $\delta$  8.30 (d,  $J = 7.8$  Hz, 1H), 7.91 (s, 1H), 7.62 (d,  $J = 1.8$  Hz, 1H), 7.21 (dd,  $J = 8.8, 1.5$  Hz, 1H), 7.16 (s, 1H), 6.65 (d,

$J = 8.9$  Hz, 1H), 4.58 (d,  $J = 4.2$  Hz, 1H), 3.50–3.42 (m, 1H), 3.31–3.24 (m, 1H), 2.80–2.71 (m, 1H), 1.96–1.91 (m, 2H), 1.83–1.78 (m, 2H), 1.36–1.23 (m, 4H), 1.18 (d,  $J = 6.8$  Hz, 6H).  $^{13}\text{C}$  NMR (75 MHz, DMSO- $d_6$ )  $\delta$  ppm 171.23, 148.65, 135.56, 132.50, 113.71, 111.88, 107.94, 92.83, 80.35, 68.22, 49.6, 33.63, 30.39, 23.35, 20.67. HRMS (ESI): calcd for  $\text{C}_{18}\text{H}_{24}\text{N}_2\text{O}_2$  [ $\text{M} + \text{H}$ ] $^+$  301.18, found 301.19. Purity: 96.54% by HPLC (MeOH/ $\text{H}_2\text{O} = 90:10$ ).  $R_f$ : 0.32 by TLC (PE/EA = 1:1). [ $\alpha$ ] $^{25}\text{D} = 0.00$  (C 1.0, MeOH).

4.2.2.2. 2-(((1R,4R)-4-hydroxycyclohexyl)amino)-5-(3,3-dimethylbut-1-yn-1-yl)benzamide (2). Compound **2** was prepared from intermediate **37** (295 mg, 1.47 mmol) according to the general procedures. White solid (272 mg, 58.9%). Mp 207.1–208.8  $^{\circ}\text{C}$ .  $^1\text{H}$  NMR (300 MHz, DMSO- $d_6$ )  $\delta$  8.28 (d,  $J = 7.6$  Hz, 1H), 7.91 (s, 1H), 7.59 (s, 1H), 7.19 (d,  $J = 8.5$  Hz, 1H), 7.13 (s, 1H), 6.64 (d,  $J = 8.8$  Hz, 1H), 4.57 (d,  $J = 4.0$  Hz, 1H), 3.50–3.42 (m, 1H), 3.29–3.24 (m, 1H), 1.96–1.93 (m, 2H), 1.83–1.79 (m, 2H), 1.36–1.32 (m, 2H), 1.26 (s, 9H), 1.19–1.09 (m, 2H). HRMS (ESI): calcd for  $\text{C}_{19}\text{H}_{26}\text{N}_2\text{O}_2$  [ $\text{M} + \text{H}$ ] $^+$  315.20, found 315.20. Purity: 99.05% by HPLC (MeOH/ $\text{H}_2\text{O} = 90:10$ ).  $R_f$ : 0.33 by TLC (PE/EA = 1:1). [ $\alpha$ ] $^{25}\text{D} = 0.00$  (C 1.0, MeOH).

4.2.2.3. 2-(((1R,4R)-4-hydroxycyclohexyl)amino)-5-(4-methylpent-1-yn-1-yl)benzamide (3). Compound **3** was prepared from intermediate **38** (272 mg, 1.35 mmol) according to the general procedures. White solid (193 mg, 45.5%). Mp 157.3–158.5  $^{\circ}\text{C}$ .  $^1\text{H}$  NMR (300 MHz, DMSO- $d_6$ )  $\delta$  8.31 (d,  $J = 7.2$  Hz, 1H), 7.91 (s, 1H), 7.65 (s, 1H), 7.25–7.17 (m, 2H), 6.65 (d,  $J = 8.7$  Hz, 1H), 4.59 (d,  $J = 3.9$  Hz, 1H), 3.50–3.41 (m, 1H), 3.32–3.21 (m, 1H), 2.28–2.26 (m, 2H), 1.96–1.93 (m, 2H), 1.83–1.79 (m, 3H), 1.33–1.15 (m, 4H), 0.99 (d,  $J = 6.5$  Hz, 6H). HRMS (ESI): calcd for  $\text{C}_{19}\text{H}_{26}\text{N}_2\text{O}_2$  [ $\text{M} + \text{H}$ ] $^+$  315.20, found 315.21. Purity: 96.87% by HPLC (MeOH/ $\text{H}_2\text{O} = 90:10$ ).  $R_f$ : 0.35 by TLC (PE/EA = 1:1). [ $\alpha$ ] $^{25}\text{D} = 0.00$  (C 1.0, MeOH).

4.2.2.4. 2-(((1R,4R)-4-hydroxycyclohexyl)amino)-5-(hex-1-yn-1-yl)benzamide (4). Compound **4** was prepared from intermediate **39** (270 mg, 1.34 mmol) according to the general procedures. White solid (166 mg, 39.3%). Mp 173.3–175.1  $^{\circ}\text{C}$ .  $^1\text{H}$  NMR (300 MHz, DMSO- $d_6$ )  $\delta$  8.30 (d,  $J = 7.6$  Hz, 1H), 7.89 (s, 1H), 7.64 (s, 1H), 7.23 (d,  $J = 8.7$  Hz, 1H), 7.13 (s, 1H), 6.65 (d,  $J = 8.8$  Hz, 1H), 4.55 (s, 1H), 3.49–3.43 (m, 1H), 3.28–3.23 (m, 1H), 2.37 (t,  $J = 6.7$  Hz, 2H),

1.97–1.93 (m, 2H), 1.83–1.79 (m, 2H), 1.55–1.38 (m, 4H), 1.36–1.25 (m, 2H), 1.23–1.12 (m, 2H), 0.91 (t,  $J = 6.9$  Hz, 3H).  $^{13}\text{C}$  NMR (75 MHz, DMSO- $d_6$ )  $\delta$  170.97, 148.39, 135.29, 132.27, 113.42, 111.64, 107.84, 87.13, 80.93, 67.96, 49.35, 33.36, 30.55, 30.12, 21.41, 18.37, 13.46. HRMS (ESI): calcd for  $\text{C}_{19}\text{H}_{26}\text{N}_2\text{O}_2$  [ $\text{M} + \text{H}$ ] $^+$  315.20, found 315.21. Purity: 98.86% by HPLC (MeOH/H $_2$ O = 90:10). R $_f$ : 0.32 by TLC (PE/EA = 1:1).  $[\alpha]^{25}\text{D} = -0.20$  (C 1.0, MeOH).

4.2.2.5. 2-(((1R,4R)-4-hydroxycyclohexyl)amino)-5-(5-chloropent-1-yn-1-yl)benzamide (5). Compound **5** was prepared from intermediate **40** (258 mg, 1.17 mmol) according to the general procedures. White solid (75 mg, 19.2%). Mp 184.0–185.7 °C.  $^1\text{H}$  NMR (300 MHz, DMSO- $d_6$ )  $\delta$  8.32 (d,  $J = 7.1$  Hz, 1H), 7.89 (s, 1H), 7.66 (s, 1H), 7.24 (d,  $J = 8.1$  Hz, 1H), 7.15 (s, 1H), 6.65 (d,  $J = 8.9$  Hz, 1H), 4.56 (d,  $J = 3.9$  Hz, 1H), 3.76 (t,  $J = 6.4$  Hz, 2H), 3.50–3.42 (m, 1H), 3.28–3.24 (m, 1H), 2.55–2.52 (m, 2H), 1.98–1.91 (m, 4H), 1.82–1.78 (m, 2H), 1.36–1.27 (m, 2H), 1.19–1.11 (m, 2H).  $^{13}\text{C}$  NMR (75 MHz, DMSO- $d_6$ )  $\delta$  170.92, 148.53, 135.32, 132.45, 113.34, 111.65, 107.36, 85.43, 81.64, 67.95, 49.32, 44.21, 33.36, 31.30, 30.11, 16.22. HRMS (ESI): calcd for  $\text{C}_{18}\text{H}_{23}\text{ClN}_2\text{O}_2$  [ $\text{M} + \text{Na}$ ] $^+$  357.14, found 357.13. Purity: 99.90% by HPLC (MeOH/H $_2$ O = 90:10). R $_f$ : 0.36 by TLC (PE/EA = 1:1).  $[\alpha]^{25}\text{D} = 0.30$  (C 1.0, MeOH).

4.2.2.6. 2-(((1R,4R)-4-hydroxycyclohexyl)amino)-5-(5-methylhex-1-yn-1-yl)benzamide (6). Compound **6** was prepared from intermediate **41** (288 mg, 1.34 mmol) according to the general procedures. White solid (240 mg, 54.6%). Mp 156.1–157.6 °C.  $^1\text{H}$  NMR (300 MHz, DMSO- $d_6$ )  $\delta$  8.29 (d,  $J = 7.5$  Hz, 1H), 7.88 (s, 1H), 7.64 (s, 1H), 7.23 (d,  $J = 8.6$  Hz, 1H), 7.12 (s, 1H), 6.66 (d,  $J = 8.8$  Hz, 1H), 4.54 (s, 1H), 3.52–3.43 (m, 1H), 3.29–3.25 (m, 1H), 2.38 (t,  $J = 7.3$  Hz, 2H), 1.97–1.93 (m, 2H), 1.84–1.80 (m, 2H), 1.76–1.65 (m, 1H), 1.43 (q,  $J = 7.2$  Hz, 2H), 1.34–1.13 (m, 4H), 0.91 (d,  $J = 6.6$  Hz, 6H). HRMS (ESI): calcd for  $\text{C}_{21}\text{H}_{30}\text{N}_2\text{O}_2$  [ $\text{M} + \text{H}$ ] $^+$  329.22, found 329.22. Purity: 97.12% by HPLC (MeOH/H $_2$ O = 90:10). R $_f$ : 0.25 by TLC (PE/EA = 1:1).  $[\alpha]^{25}\text{D} = -0.10$  (C 1.0, MeOH).

4.2.2.7. 2-(((1R,4R)-4-hydroxycyclohexyl)amino)-5-(cyclopropylethynyl)benzamide (7). Compound **7** was prepared from intermediate **42** (270 mg, 1.46 mmol) according to the general procedures. White solid (260 mg, 59.7%). Mp 218.8–220.4 °C.  $^1\text{H}$  NMR (300 MHz, DMSO- $d_6$ )  $\delta$  8.31 (d,  $J = 7.6$  Hz, 1H), 7.87 (s, 1H), 7.63 (s, 1H), 7.21 (d,  $J = 8.3$  Hz, 1H), 7.14 (s, 1H), 6.64 (d,  $J = 8.8$  Hz, 1H), 4.56 (d,  $J = 4.0$  Hz, 1H), 3.50–3.42 (m, 1H), 3.29–3.22 (m, 1H), 1.95–1.91 (m, 2H), 1.82–1.78 (m, 2H), 1.52–1.44 (m, 1H), 1.36–1.24 (m, 2H), 1.23–1.11 (m, 2H), 0.86–0.80 (m, 2H), 0.68–0.63 (m, 2H). HRMS (ESI): calcd for  $\text{C}_{18}\text{H}_{22}\text{N}_2\text{O}_2$  [ $\text{M} + \text{H}$ ] $^+$  299.17, found 299.18. Purity: 96.62% by HPLC (MeOH/H $_2$ O = 90:10). R $_f$ : 0.25 by TLC (PE/EA = 1:1).  $[\alpha]^{25}\text{D} = 0.30$  (C 1.0, MeOH).

4.2.2.8. 2-(((1R,4R)-4-hydroxycyclohexyl)amino)-5-(cyclopentylethynyl)benzamide (8). Compound **8** was prepared from intermediate **43** (266 mg, 1.25 mmol) according to the general procedures. White solid (227 mg, 55.7%). Mp 208.8–210.6 °C.  $^1\text{H}$  NMR (300 MHz, DMSO- $d_6$ )  $\delta$  8.29 (d,  $J = 7.6$  Hz, 1H), 7.90 (s, 1H), 7.62 (s, 1H), 7.21 (d,  $J = 8.4$  Hz, 1H), 7.14 (s, 1H), 6.64 (d,  $J = 8.9$  Hz, 1H), 4.57 (d,  $J = 3.5$  Hz, 1H), 3.49–3.43 (m, 1H), 3.29–3.24 (m, 1H), 2.85–2.75 (m, 1H), 1.96–1.92 (m, 4H), 1.82–1.79 (m, 2H), 1.70–1.66 (m, 2H), 1.61–1.55 (m, 4H), 1.36–1.25 (m, 2H), 1.23–1.11 (m, 2H). HRMS (ESI): calcd for  $\text{C}_{20}\text{H}_{26}\text{N}_2\text{O}_2$  [ $\text{M} + \text{H}$ ] $^+$  327.20, found 327.21. Purity: 97.66% by HPLC (MeOH/H $_2$ O = 90:10). R $_f$ : 0.34 by TLC (PE/EA = 1:1).  $[\alpha]^{25}\text{D} = -0.10$  (C 1.0, MeOH).

4.2.2.9. 2-(((1R,4R)-4-hydroxycyclohexyl)amino)-5-(cyclohexylethynyl)benzamide (9). Compound **9** was prepared from intermediate **44** (322 mg, 1.42 mmol) according to the general procedures. White solid (236 mg, 48.8%). Mp 191.6–193.5 °C.  $^1\text{H}$  NMR (300 MHz, DMSO- $d_6$ )  $\delta$  8.30–8.28 (m, 1H), 7.91 (s, 1H), 7.61 (s, 1H), 7.21 (d,  $J = 8.6$  Hz, 1H), 7.14 (s, 1H), 6.65–6.63 (m, 1H), 4.58–4.56 (m, 1H), 3.50–3.40 (m, 1H), 3.29–3.23 (m, 1H), 2.61–2.55 (m, 1H), 1.95–1.91 (m, 2H), 1.81–1.78 (m, 4H), 1.70–1.63

(s, 2H), 1.50–1.10 (m, 10H). HRMS (ESI): calcd for  $\text{C}_{21}\text{H}_{28}\text{N}_2\text{O}_2$  [ $\text{M} + \text{H}$ ] $^+$  341.22, found 341.22. Purity: 97.59% by HPLC (MeOH/H $_2$ O = 90:10). R $_f$ : 0.37 by TLC (PE/EA = 1:1).  $[\alpha]^{25}\text{D} = -0.20$  (C 1.0, MeOH).

4.2.3. General Procedure for the Intermediate 2-(((1R,4R)-4-hydroxycyclohexyl)amino)-5-iodobenzamide (45). **35** (1 equiv) was dissolved in DMSO, followed by addition of *trans*-4-aminocyclohexanol (4.5 equiv) and DIPEA (9 equiv) and stirred for 16 h at 120 °C. After the reaction was finished, the mixture was poured into water (60 ml) and extracted with ethyl acetate (60 ml  $\times$  2). Finally, the EA layer was washed with brine (30 ml  $\times$  3), dried over anhydrous sodium sulfate, and concentrated under reduced pressure to afford the residue. The residue was dissolved in EtOH (30 ml) and DMSO (5 ml). NaOH (2 M, 4 ml) and 30% H $_2$ O $_2$  (3 ml) were added. Reaction was stirred at 30 °C for 12 h. EtOH was removed under reduced pressure after the reaction was completed. The residue was dissolved in EA (50 ml) and washed with water (50 ml  $\times$  2) and brine (30 mL  $\times$  3), dried over anhydrous Na $_2$ SO $_4$  and concentrated in vacuo. The residue was purified by silica gel column chromatography (PE/EA, 2:1) to afford intermediate **45**. Intermediate **45** was prepared from **35** (987.0 mg, 4.0 mmol) according to the general procedures. Light yellow solid (731 mg, 50.8%).  $^1\text{H}$  NMR (300 MHz, DMSO- $d_6$ )  $\delta$  8.04 (d,  $J = 7.7$  Hz, 1H), 7.80 (s, 1H), 7.74 (d,  $J = 2.2$  Hz, 1H), 7.37 (dd,  $J = 8.8, 2.1$  Hz, 1H), 7.10 (s, 1H), 6.47 (d,  $J = 9.0$  Hz, 1H), 4.47 (d,  $J = 4.3$  Hz, 1H), 3.44–3.29 (m, 1H), 3.20–3.11 (s, 1H), 1.86–1.82 (m, 2H), 1.73–1.68 (m, 2H), 1.28–0.98 (m, 4H).

4.2.4. General Procedure for the compounds 10–11. The method used for the synthesis of compounds **10–11** is similar to the one used for the synthesis of compounds **1–9**.

4.2.4.1.2-(((1R,4R)-4-hydroxycyclohexyl)amino)-5-(3-(dimethylamino)prop-1-yn-1-yl)benzamide (10). Compound **10** was prepared from intermediate **45** (270 mg, 0.75 mmol) and *N,N*-dimethylprop-2-yn-1-amine (125 mg, 1.5 mmol) according to the general procedures. Light yellow solid (67 mg, 28.3%). Mp 189.4–190.9 °C.  $^1\text{H}$  NMR (300 MHz, DMSO- $d_6$ )  $\delta$  8.30–8.25 (m, 1H), 7.84 (s, 1H), 7.61 (s, 1H), 7.19–7.16 (m, 1H), 7.10 (s, 1H), 6.61–6.56 (m, 1H), 4.50 (s, 1H), 3.42–3.30 (m, 3H), 3.21–3.14 (m, 1H), 2.16 (s, 6H), 1.87–1.83 (m, 2H), 1.73–1.69 (m, 2H), 1.23–1.06 (m, 4H). HRMS (ESI): calcd for  $\text{C}_{18}\text{H}_{25}\text{N}_3\text{O}_2$  [ $\text{M} + \text{H}$ ] $^+$  316.19, found 316.20. Purity: 96.62% by HPLC (MeOH/H $_2$ O = 90:10). R $_f$ : 0.34 by TLC (DCM/MEOH = 4:1).  $[\alpha]^{25}\text{D} = 0.10$  (C 1.0, MeOH).

4.2.4.2.2-(((1R,4R)-4-hydroxycyclohexyl)amino)-5-(3-(diethylamino)prop-1-yn-1-yl) benzamide (11). Compound **11** was prepared from intermediate **45** (360 mg, 1 mmol) and *N,N*-diethylprop-2-yn-1-amine (222 mg, 2 mmol) according to the general procedures. Hazel solid (144 mg, 42.0%). Mp 196.9–197.9 °C.  $^1\text{H}$  NMR (300 MHz, DMSO- $d_6$ )  $\delta$  8.37 (d,  $J = 8.0$  Hz, 1H), 7.88 (s, 1H), 7.67 (s, 1H), 7.24 (d,  $J = 9.2$  Hz, 1H), 7.18 (s, 1H), 6.62 (d,  $J = 8.9$  Hz, 1H), 4.55 (s, 1H), 4.03 (s, 2H), 2.97 (d,  $J = 7.5$  Hz, 4H), 2.41 (s, 2H), 1.84 (d,  $J = 16.0$  Hz, 2H), 1.71 (d,  $J = 11.7$  Hz, 2H), 1.31–1.15 (m, 4H), 1.12 (t,  $J = 7.0$  Hz, 6H).  $^{13}\text{C}$  NMR (75 MHz, DMSO)  $\delta$  170.91, 148.63, 135.49, 132.52, 113.37, 111.66, 107.07, 84.97, 81.87, 67.95, 49.30, 46.54, 41.02, 33.36, 30.08, 12.49. HRMS (ESI): calcd for  $\text{C}_{20}\text{H}_{29}\text{N}_3\text{O}_2$  [ $\text{M} + \text{H}$ ] $^+$  344.23, found 344.23. Purity: 98.00% by HPLC (MeOH/H $_2$ O = 90:10). R $_f$ : 0.32 by TLC (DCM/MEOH = 4:1).  $[\alpha]^{25}\text{D} = 0.40$  (C 1.0, MeOH).

4.2.5. General Procedure for the compounds 12–23 and intermediates 46–48. The method used for the synthesis of compounds **12–23** and intermediates **46–48** is similar to the one used for the synthesis of compounds **1–9**.

4.2.5.1.2-((2-hydroxyethyl)amino)-5-(hex-1-yn-1-yl)benzamide (12). Compound **12** was prepared from intermediate **39** (201 mg, 1.0 mmol) and 2-aminoethan-1-ol (275 mg, 4.5 mmol) according to the general procedures. White solid (92 mg, 35.4%). Mp

81.5–82.8 °C.  $^1\text{H}$  NMR (300 MHz, DMSO- $d_6$ )  $\delta$  8.26 (t,  $J$  = 5.2 Hz, 1H), 7.81 (s, 1H), 7.54 (s, 1H), 7.15 (d,  $J$  = 8.1 Hz, 1H), 7.06 (s, 1H), 6.52 (d,  $J$  = 8.3 Hz, 1H), 4.70 (t,  $J$  = 4.8 Hz, 1H), 3.50–3.44 (m, 2H), 3.09–3.04 (m, 2H), 2.28 (t,  $J$  = 6.2 Hz, 2H), 1.42–1.29 (m, 4H), 0.81 (t,  $J$  = 7.0 Hz, 3H). HRMS (ESI): calcd for  $\text{C}_{15}\text{H}_{20}\text{N}_2\text{O}_2$  [M + Na] $^+$  283.15, found 283.14. Purity: 99.26% by HPLC (MeOH/H $_2$ O = 90:10). R $_f$ : 0.25 by TLC (PE/EA = 1:1).

4.2.5.2.2-((2-methoxyethyl)amino)-5-(hex-1-yn-1-yl)benzamide (13). Compound **13** was prepared from intermediate **39** (201 mg, 1.0 mmol) and 2-methoxyethan-1-amine (337 mg, 4.5 mmol) according to the general procedures. White solid (105 mg, 38.3%). Mp 83.6–85.1 °C.  $^1\text{H}$  NMR (300 MHz, chloroform- $d$ )  $\delta$  8.09 (s, 1H), 7.47 (s, 1H), 7.36 (d,  $J$  = 8.6 Hz, 1H), 6.64 (d,  $J$  = 8.6 Hz, 1H), 5.76 (brs, 2H), 3.64 (t,  $J$  = 5.5 Hz, 2H), 3.42 (s, 3H), 3.38–3.37 (m, 2H), 2.40 (t,  $J$  = 6.8 Hz, 2H), 1.63–1.54 (m, 2H), 1.52–1.44 (m, 2H), 0.96 (t,  $J$  = 7.1 Hz, 3H). HRMS (ESI): calcd for  $\text{C}_{16}\text{H}_{22}\text{N}_2\text{O}_2$  [M + Na] $^+$  297.17, found 297.16. Purity: 99.22% by HPLC (MeOH/H $_2$ O = 90:10). R $_f$ : 0.25 by TLC (PE/EA = 2:1).

4.2.5.3.2-((2-ethoxyethyl)amino)-5-(hex-1-yn-1-yl)benzamide (14). Compound **14** was prepared from intermediate **39** (201 mg, 1.0 mmol) and 2-ethoxyethan-1-amine (401 mg, 4.5 mmol) according to the general procedures. White solid (105 mg, 38.3%). White solid (218 mg, 75.6%). Mp 96.5–97.8 °C.  $^1\text{H}$  NMR (300 MHz, chloroform- $d$ )  $\delta$  8.09 (s, 1H), 7.47–7.46 (m, 1H), 7.35 (dd,  $J$  = 8.8, 1.8 Hz, 1H), 6.64 (d,  $J$  = 8.8 Hz, 1H), 5.71 (brs, 2H), 3.68 (t,  $J$  = 5.7 Hz, 2H), 3.57 (q,  $J$  = 7.0 Hz, 2H), 3.38 (t,  $J$  = 5.5 Hz, 2H), 2.40 (t,  $J$  = 6.9 Hz, 2H), 1.63–1.54 (m, 2H), 1.52–1.42 (m, 2H), 1.25 (t,  $J$  = 7.0 Hz, 3H), 0.96 (t,  $J$  = 7.2 Hz, 3H). HRMS (ESI): calcd for  $\text{C}_{17}\text{H}_{24}\text{N}_2\text{O}_2$  [M + Na] $^+$  311.18, found 311.17. Purity: 96.97% by HPLC (MeOH/H $_2$ O = 90:10). R $_f$ : 0.3 by TLC (PE/EA = 2:1).

4.2.5.4.2-((3-hydroxypropyl)amino)-5-(hex-1-yn-1-yl)benzamide (15). Compound **15** was prepared from intermediate **39** (201 mg, 1.0 mmol) and 3-aminopropan-1-ol (338 mg, 4.5 mmol) according to the general procedures. White solid (105 mg, 38.3%). White solid (127 mg, 46.3%). Mp 124.7–126.5 °C.  $^1\text{H}$  NMR (300 MHz, DMSO- $d_6$ )  $\delta$  8.31 (t,  $J$  = 5.2 Hz, 1H), 7.92 (s, 1H), 7.65–7.64 (m, 1H), 7.27–7.23 (m, 1H), 7.19 (s, 1H), 6.62 (d,  $J$  = 8.7 Hz, 1H), 4.56 (t,  $J$  = 5.1 Hz, 1H), 3.48 (q,  $J$  = 5.9 Hz, 2H), 3.16 (q,  $J$  = 6.4 Hz, 2H), 2.37 (t,  $J$  = 6.6 Hz, 2H), 1.73–1.64 (m, 2H), 1.54–1.36 (m, 4H), 0.91 (t,  $J$  = 7.0 Hz, 3H). HRMS (ESI): calcd for  $\text{C}_{16}\text{H}_{22}\text{N}_2\text{O}_2$  [M + Na] $^+$  297.17, found 297.16. Purity: 97.65% by HPLC (MeOH/H $_2$ O = 90:10). R $_f$ : 0.5 by TLC (DCM/MeOH = 20:1).

4.2.5.5.2-((3-methoxypropyl)amino)-5-(hex-1-yn-1-yl)benzamide (16). Compound **16** was prepared from intermediate **39** (201 mg, 1.0 mmol) and 3-methoxypropan-1-amine (401 mg, 4.5 mmol) according to the general procedures. Light yellow solid (185 mg, 64.2%). Mp 86.8–88.5 °C.  $^1\text{H}$  NMR (300 MHz, chloroform- $d$ )  $\delta$  8.00 (s, 1H), 7.46–7.45 (m, 1H), 7.37–7.33 (m, 1H), 6.65 (d,  $J$  = 8.5 Hz, 1H), 5.67 (brs, 2H), 3.50 (t,  $J$  = 5.9 Hz, 2H), 3.37 (s, 3H), 3.31–3.27 (m, 2H), 2.40 (t,  $J$  = 6.7 Hz, 2H), 1.97–1.88 (m, 2H), 1.61–1.54 (m, 2H), 1.51–1.44 (m, 2H), 0.96 (t,  $J$  = 7.1 Hz, 3H). HRMS (ESI): calcd for  $\text{C}_{17}\text{H}_{24}\text{N}_2\text{O}_2$  [M + Na] $^+$  311.18, found 311.17. Purity: 99.18% by HPLC (MeOH/H $_2$ O = 90:10). R $_f$ : 0.3 by TLC (PE/EA = 2:1).

4.2.5.6.2-((3-ethoxypropyl)amino)-5-(hex-1-yn-1-yl)benzamide (17). Compound **17** was prepared from intermediate **39** (201 mg, 1.0 mmol) and 3-ethoxypropan-1-amine (464 mg, 4.5 mmol) according to the general procedures. Light yellow solid (159 mg, 52.6%). Mp 75.7–76.9 °C.  $^1\text{H}$  NMR (300 MHz, chloroform- $d$ )  $\delta$  7.99 (s, 1H), 7.46 (s, 1H), 7.35 (d,  $J$  = 8.6 Hz, 1H), 6.66 (d,  $J$  = 8.5 Hz, 1H), 5.65 (brs, 2H), 3.56–3.47 (m, 4H), 3.33–3.28 (m, 2H), 2.40 (t,  $J$  = 6.9 Hz, 2H), 1.97–1.89 (m, 2H), 1.64–1.55 (m, 2H), 1.52–1.45 (m, 2H), 1.23 (t,  $J$  = 6.9 Hz, 3H), 0.96 (t,  $J$  = 7.0 Hz, 3H).  $^{13}\text{C}$  NMR (75 MHz, DMSO- $d_6$ )  $\delta$  170.88, 149.20, 135.33, 132.10, 113.66, 111.03, 108.08, 87.22, 80.90, 67.28, 65.34, 30.54, 28.88, 21.41, 18.37, 15.04, 13.47. HRMS (ESI): calcd for  $\text{C}_{18}\text{H}_{26}\text{N}_2\text{O}_2$  [M + Na] $^+$  325.20,

found 325.19. Purity: 99.21% by HPLC (MeOH/H $_2$ O = 90:10). R $_f$ : 0.4 by TLC (PE/EA = 2:1).

4.2.5.7.2-((2-acetamidoethyl)amino)-5-(hex-1-yn-1-yl)benzamide (18). Compound **18** was prepared from intermediate **39** (201 mg, 1.0 mmol) and N-(2-aminoethyl)acetamide (459 mg, 4.5 mmol) according to the general procedures. White solid (159 mg, 52.8%). Mp 141.2–143.6 °C.  $^1\text{H}$  NMR (300 MHz, DMSO- $d_6$ )  $\delta$  8.25 (s, 1H), 7.92 (s, 1H), 7.82 (s, 1H), 7.56 (s, 1H), 7.16 (d,  $J$  = 8.8 Hz, 1H), 7.10 (s, 1H), 6.60 (d,  $J$  = 8.7 Hz, 1H), 3.14–3.04 (m, 4H), 2.28 (t,  $J$  = 6.5 Hz, 2H), 1.71 (s, 3H), 1.45–1.29 (m, 4H), 0.81 (t,  $J$  = 7.0 Hz, 3H).  $^{13}\text{C}$  NMR (75 MHz, DMSO- $d_6$ )  $\delta$  170.79, 169.49, 149.04, 135.28, 132.13, 113.91, 111.10, 108.31, 87.32, 80.85, 41.33, 37.95, 30.52, 22.53, 21.42, 18.36, 13.49. HRMS (ESI): calcd for  $\text{C}_{17}\text{H}_{23}\text{N}_3\text{O}_2$  [M + Na] $^+$  324.19, found 324.17. Purity: 99.37% by HPLC (MeOH/H $_2$ O = 90:10). R $_f$ : 0.3 by TLC (PE/EA = 2:1).

4.2.5.8.2-((tetrahydrofuran-3-yl)amino)-5-(hex-1-yn-1-yl)benzamide (19). Compound **19** was prepared from intermediate **39** (201 mg, 1.0 mmol) and tetrahydrofuran-3-amine (392 mg, 4.5 mmol) according to the general procedures. White solid (98 mg, 34.2%). Mp 153.0–154.8 °C.  $^1\text{H}$  NMR (300 MHz, chloroform- $d$ )  $\delta$  8.14–8.12 (m, 1H), 7.47–7.46 (m, 1H), 7.37–7.34 (m, 1H), 6.58 (d,  $J$  = 8.7 Hz, 1H), 5.74 (brs, 2H), 4.13–4.01 (m, 2H), 3.99–3.86 (m, 2H), 3.72–3.68 (m, 1H), 2.39 (t,  $J$  = 6.9 Hz, 2H), 2.33–2.24 (m, 1H), 1.96–1.87 (m, 1H), 1.63–1.42 (m, 4H), 0.94 (t,  $J$  = 7.1 Hz, 3H). HRMS (ESI): calcd for  $\text{C}_{17}\text{H}_{22}\text{N}_2\text{O}_2$  [M + Na] $^+$  309.17, found 309.16. Purity: 98.23% by HPLC (MeOH/H $_2$ O = 90:10). R $_f$ : 0.25 by TLC (PE/EA = 2:1).

4.2.5.9.2-(((tetrahydrofuran-3-yl)methyl)amino)-5-(hex-1-yn-1-yl)benzamide (20). Compound **20** was prepared from intermediate **39** (201 mg, 1.0 mmol) and (tetrahydrofuran-3-yl)methanamine (455 mg, 4.5 mmol) according to the general procedures. White solid (176 mg, 58.6%). Mp 138.5–139.9 °C.  $^1\text{H}$  NMR (300 MHz, DMSO- $d_6$ )  $\delta$  8.35 (s, 1H), 7.85 (s, 1H), 7.58–7.57 (m, 1H), 7.18–7.15 (m, 1H), 7.11 (s, 1H), 6.57–6.54 (m, 1H), 3.67–3.62 (m, 2H), 3.58–3.50 (m, 1H), 3.35–3.30 (m, 1H), 3.03–2.99 (m, 2H), 2.30–2.26 (m, 2H), 1.94–1.86 (m, 1H), 1.55–1.45 (m, 2H), 1.43–1.29 (m, 4H), 0.84–0.79 (m, 3H). HRMS (ESI): calcd for  $\text{C}_{18}\text{H}_{24}\text{N}_2\text{O}_2$  [M + Na] $^+$  323.18, found 323.17. Purity: 99.55% by HPLC (MeOH/H $_2$ O = 90:10). R $_f$ : 0.2 by TLC (PE/EA = 2:1).

4.2.5.10.2-((tetrahydro-2H-pyran-4-yl)amino)-5-(hex-1-yn-1-yl)benzamide (21). Compound **21** was prepared from intermediate **39** (201 mg, 1.0 mmol) and tetrahydro-2H-pyran-4-amine (455 mg, 4.5 mmol) according to the general procedures. White solid (165 mg, 55%). Mp 182.1–183.9 °C.  $^1\text{H}$  NMR (300 MHz, DMSO- $d_6$ )  $\delta$  8.32 (d,  $J$  = 7.6 Hz, 1H), 7.84 (s, 1H), 7.57 (s, 1H), 7.14 (d,  $J$  = 8.5 Hz, 1H), 7.10 (s, 1H), 6.62 (d,  $J$  = 8.8 Hz, 1H), 3.73 (d,  $J$  = 12.0 Hz, 2H), 3.54–3.45 (m, 1H), 3.36 (t,  $J$  = 10.7 Hz, 2H), 2.28 (t,  $J$  = 6.7 Hz, 2H), 1.83–1.79 (m, 2H), 1.45–1.21 (m, 6H), 0.81 (t,  $J$  = 7.1 Hz, 3H).  $^{13}\text{C}$  NMR (75 MHz, DMSO- $d_6$ )  $\delta$  170.93, 147.97, 135.29, 132.31, 113.60, 111.74, 108.20, 87.28, 80.84, 65.53, 46.95, 32.67, 30.52, 21.42, 18.36, 13.48. HRMS (ESI): calcd for  $\text{C}_{17}\text{H}_{24}\text{N}_2\text{O}_2$  [M + H] $^+$  301.18, found 301.19. Purity: 96.51% by HPLC (MeOH/H $_2$ O = 90:10). R $_f$ : 0.3 by TLC (PE/EA = 2:1).

4.2.5.11.2-(((tetrahydro-2H-pyran-4-yl)methyl)amino)-5-(hex-1-yn-1-yl)benzamide (22). Compound **22** was prepared from intermediate **39** (201 mg, 1.0 mmol) and (tetrahydro-2H-pyran-4-yl)methanamine (518 mg, 4.5 mmol) according to the general procedures. White solid (137 mg, 43.6%). Mp 150.3–151.9 °C.  $^1\text{H}$  NMR (300 MHz, chloroform- $d$ )  $\delta$  8.04 (s, 1H), 7.37–7.36 (m, 1H), 7.26 (dd,  $J$  = 8.7, 2.0 Hz, 1H), 6.52 (d,  $J$  = 8.8 Hz, 1H), 5.60 (brs, 2H), 3.91 (dd,  $J$  = 11.1, 3.2 Hz, 2H), 3.31 (t,  $J$  = 11.0 Hz, 2H), 2.99 (d,  $J$  = 6.2 Hz, 2H), 2.31 (t,  $J$  = 6.9 Hz, 2H), 1.84–1.76 (m, 1H), 1.67–1.62 (m, 2H), 1.54–1.23 (m, 6H), 0.87 (t,  $J$  = 7.1 Hz, 3H). HRMS (ESI): calcd for  $\text{C}_{19}\text{H}_{26}\text{N}_2\text{O}_2$  [M + Na] $^+$  337.20, found 337.19. Purity: 99.34% by HPLC (MeOH/H $_2$ O = 90:10). R $_f$ : 0.25 by TLC (PE/EA = 2:1).

4.2.5.12.2-((1-acetylpiperidin-4-yl)amino)-5-(hex-1-yn-1-yl)

benzamide (23). Compound **23** was prepared from intermediate **39** (201 mg, 1.0 mmol) and 1-(4-aminopiperidin-1-yl)ethan-1-one (639 mg, 4.5 mmol) according to the general procedures. White solid (102 mg, 29.9%). Mp 165.1–166.4 °C. <sup>1</sup>H NMR (300 MHz, DMSO-*d*<sub>6</sub>) δ 8.34 (d, *J* = 7.3 Hz, 1H), 7.83 (s, 1H), 7.58 (s, 1H), 7.16 (d, *J* = 7.7 Hz, 1H), 7.10 (s, 1H), 6.64 (d, *J* = 8.3 Hz, 1H), 4.03–3.99 (m, 1H), 3.64–3.52 (m, 2H), 3.17–3.09 (m, 1H), 2.84–2.76 (m, 1H), 2.30–2.26 (m, 2H), 1.91 (s, 3H), 1.82–1.75 (m, 2H), 1.43–1.23 (m, 4H), 1.11–1.08 (m, 2H), 0.83–0.79 (m, 3H). HRMS (ESI): calcd for C<sub>18</sub>H<sub>25</sub>N<sub>3</sub>O [M + H]<sup>+</sup> 364.21, found 364.20. Purity: 95.35% by HPLC (MeOH/H<sub>2</sub>O = 90:10). R<sub>f</sub>: 0.3 by TLC (PE/EA = 2:1).

4.2.5.13. *tert*-butyl 4-((2-carbamoyl-4-(hex-1-yn-1-yl)phenyl)amino)piperidine-1-carboxylate (46). Intermediate **46** was prepared from intermediate **39** (2.41 g, 12.0 mmol) and *tert*-butyl 4-aminopiperidine-1-carboxylate (10.81 g, 54 mmol) according to the general procedures. White solid (3.0 g, 62.6%). <sup>1</sup>H NMR (300 MHz, DMSO-*d*<sub>6</sub>) δ 8.42 (d, *J* = 7.6 Hz, 1H), 7.94 (s, 1H), 7.67 (s, *J* = 2.1 Hz, 1H), 7.24 (d, *J* = 9.0 Hz, 1H), 7.18 (s, 1H), 6.71 (d, *J* = 8.7 Hz, 1H), 3.80–3.76 (m, 2H), 3.09–2.92 (m, 2H), 2.37 (t, *J* = 6.8 Hz, 2H), 1.91–1.87 (m, 2H), 1.55–1.41 (m, 4H), 1.40 (s, 9H), 1.26–1.19 (m, 2H), 0.91 (t, *J* = 7.0 Hz, 3H).

4.2.5.14. *tert*-butyl 4-(((2-carbamoyl-4-(hex-1-yn-1-yl)phenyl)amino)methyl)piperidine-1-carboxylate (47). Intermediate **47** was prepared from intermediate **39** (402 mg, 2.0 mmol) and *tert*-butyl 4-(aminomethyl)piperidine-1-carboxylate (1.93 g, 9.0 mmol) according to the general procedures. Light yellow solid (673 mg, 81.4%). <sup>1</sup>H NMR (300 MHz, DMSO-*d*<sub>6</sub>) δ 8.44 (t, *J* = 5.5 Hz, 1H), 7.91 (s, 1H), 7.64 (s, 1H), 7.22 (d, *J* = 8.5 Hz, 1H), 7.15 (s, 1H), 6.62 (d, *J* = 8.8 Hz, 1H), 3.95–3.91 (m, 2H), 3.03–2.99 (m, 2H), 2.77–2.59 (m, 2H), 2.35 (t, *J* = 6.7 Hz, 2H), 1.67–1.64 (m, 3H), 1.56–1.41 (m, 4H), 1.37 (s, 9H), 1.11–0.98 (s, 2H), 0.89 (t, *J* = 7.0 Hz, 3H).

4.2.5.15. *tert*-butyl 3-((2-carbamoyl-4-(hex-1-yn-1-yl)phenyl)amino)piperidine-1-carboxylate (48). Intermediate **48** was prepared from intermediate **39** (402 mg, 2.0 mmol) and *tert*-butyl 3-aminopiperidine-1-carboxylate (1.80 g, 9 mmol) according to the general procedures. Light yellow oil (713 mg, 89.3%). <sup>1</sup>H NMR (300 MHz, chloroform-*d*) δ 8.04 (d, *J* = 7.0 Hz, 1H), 7.46 (s, 1H), 7.34 (dd, *J* = 8.6, 2.0 Hz, 1H), 6.74 (d, *J* = 8.8 Hz, 1H), 5.72 (brs, 2H), 3.88–3.83 (m, 1H), 3.45–3.34 (m, 1H), 2.98–2.90 (m, 1H), 2.83–2.66 (m, 1H), 2.39 (t, *J* = 6.9 Hz, 2H), 2.14–2.08 (m, 1H), 1.83–1.48 (m, 8H), 1.46 (s, 9H), 0.95 (t, *J* = 7.1 Hz, 3H).

4.2.6. General Procedure for the compounds 24–26. Silica gel (10 equiv) was added to a mixture of appropriate intermediate **46–48** (1 equiv) in toluene and stirred at 100 °C for 48 h. After the reaction was completed, it was concentrated and purified directly by silica gel column chromatography (DCM/MeOH = 30:1–10:1) to give title compounds **24–26**.

4.2.6.1.2-(piperidin-4-ylamino)-5-(hex-1-yn-1-yl)benzamide (24). Compound **24** was prepared from intermediate **46** (3 g, 7.5 mmol) and silica gel (4.51 g, 75 mmol) according to the general procedures. White solid (2.1 g, 93.6%). Mp 183.2–183.9 °C. <sup>1</sup>H NMR (300 MHz, DMSO-*d*<sub>6</sub>) δ 8.39 (d, *J* = 7.5 Hz, 1H), 7.92 (s, 1H), 7.65 (s, 1H), 7.22 (d, *J* = 8.4 Hz, 1H), 7.18 (s, 1H), 6.67 (d, *J* = 8.7 Hz, 1H), 3.47–3.38 (m, 1H), 2.95–2.90 (m, 2H), 2.59 (t, *J* = 11.0 Hz, 2H), 2.37 (t, *J* = 6.5 Hz, 2H), 1.88–1.84 (m, 2H), 1.52–1.38 (m, 4H), 1.26–1.22 (m, 2H), 0.91 (t, *J* = 7.0 Hz, 3H). <sup>13</sup>C NMR (75 MHz, DMSO-*d*<sub>6</sub>) δ 170.96, 148.08, 135.28, 132.31, 113.43, 111.63, 107.87, 87.17, 80.90, 48.45, 44.46, 33.01, 30.54, 21.42, 18.36, 13.48. HRMS (ESI): calcd for C<sub>18</sub>H<sub>25</sub>N<sub>3</sub>O [M + H]<sup>+</sup> 300.20, found 300.21. Purity: 95.35% by HPLC (MeOH/H<sub>2</sub>O = 90:10). R<sub>f</sub>: 0.3 by TLC (PE/EA = 1:1).

4.2.6.2.2-((piperidin-4-ylmethyl)amino)-5-(hex-1-yn-1-yl)benzamide (25). Compound **25** was prepared from intermediate **47** (673 mg, 1.63 mmol) and silica gel (979 mg, 16.3 mmol) according to the general procedures. White solid (356 mg, 69.7%). Mp 159.0–160.8 °C. <sup>1</sup>H NMR (300 MHz, Methanol-*d*<sub>4</sub>) δ 7.62 (s, 1H), 7.29

(d, *J* = 9.5 Hz, 1H), 6.67 (d, *J* = 8.9 Hz, 1H), 3.13–3.03 (m, 4H), 2.61 (t, *J* = 12.2 Hz, 2H), 2.38 (t, *J* = 6.6 Hz, 2H), 1.85–1.81 (m, 3H), 1.61–1.46 (m, 4H), 1.28–1.18 (m, 2H), 0.97 (t, *J* = 7.2 Hz, 3H). HRMS (ESI): calcd for C<sub>19</sub>H<sub>27</sub>N<sub>3</sub>O [M + H]<sup>+</sup> 314.22, found 314.22. Purity: 95.21% by HPLC (MeOH/H<sub>2</sub>O = 90:10). R<sub>f</sub>: 0.25 by TLC (PE/EA = 1:1).

4.2.6.3.2-(piperidin-3-ylamino)-5-(hex-1-yn-1-yl)benzamide (26). Compound **26** was prepared from intermediate **48** (713 mg, 1.79 mmol) and silica gel (1.08 g, 17.9 mmol) according to the general procedures. Light yellow solid (271 mg, 50.6%). Mp 106.1–108.4 °C. <sup>1</sup>H NMR (300 MHz, Methanol-*d*<sub>4</sub>) δ 7.62 (s, 1H), 7.28 (d, *J* = 8.7 Hz, 1H), 6.74 (d, *J* = 8.8 Hz, 1H), 3.52–3.42 (m, 1H), 3.23–3.19 (m, 1H), 2.96–2.92 (m, 1H), 2.61 (t, *J* = 11.7 Hz, 1H), 2.44–2.36 (m, 3H), 2.13–2.09 (m, 1H), 1.82–1.77 (m, 1H), 1.67–1.41 (m, 6H), 0.97 (t, *J* = 6.6 Hz, 3H). HRMS (ESI): calcd for C<sub>18</sub>H<sub>25</sub>N<sub>3</sub>O [M + H]<sup>+</sup> 300.20, found 300.21. Purity: 96.33% by HPLC (MeOH/H<sub>2</sub>O = 90:10). R<sub>f</sub>: 0.4 by TLC (PE/EA = 2:1).

4.2.7. General Procedure for the compounds 27–34. A mixture of appropriate compound (**24–26**, 1 equiv), certain acid (1.5 equiv), Bop (1.5 equiv), and DIPEA (3 equiv) in DMF were stirred at room temperature for 4 h. After the completion of reaction, the residue was obtained by concentration under reduced pressure and dissolved in EA (20 ml). The organic phase was washed with water (20 ml × 2) and saturated NaCl solution (20 ml × 2). The organic layer was dried over anhydrous Na<sub>2</sub>SO<sub>4</sub>, filtered and the solvent was evaporated to dryness under reduced pressure. Finally, the compounds **27–34** were obtained by silica gel column chromatography (PE/EA = 2:1).

4.2.7.1 2-((1-(cyclopropanecarbonyl)piperidin-4-yl)amino)-5-(hex-1-yn-1-yl)benzamide (27). Compound **27** was prepared from **24** (150 mg, 0.5 mmol) and cyclopropanecarboxylic acid (86 mg, 1.0 mmol) according to the general procedures. White solid (121 mg, 65.9%). Mp 144.5–145.8 °C. <sup>1</sup>H NMR (300 MHz, DMSO-*d*<sub>6</sub>) δ 8.43 (d, *J* = 7.2 Hz, 1H), 7.92 (s, 1H), 7.65 (s, 1H), 7.24 (d, *J* = 9.7 Hz, 1H), 7.19 (s, 1H), 6.73 (d, *J* = 9.1 Hz, 1H), 4.12–4.07 (m, 2H), 3.68–3.59 (m, 1H), 3.39–3.35 (m, 1H), 2.95–2.88 (m, 1H), 2.36 (t, *J* = 6.6 Hz, 2H), 2.01–1.92 (m, 3H), 1.53–1.37 (m, 4H), 1.22–1.13 (m, 2H), 0.89 (t, *J* = 6.9 Hz, 3H), 0.68–0.66 (m, *J* = 7.8 Hz, 4H). HRMS (ESI): calcd for C<sub>22</sub>H<sub>29</sub>N<sub>3</sub>O<sub>2</sub> [M + Na]<sup>+</sup> 390.23, found 390.22. Purity: 97.97% by HPLC (MeOH/H<sub>2</sub>O = 90:10). R<sub>f</sub>: 0.2 by TLC (PE/EA = 2:1).

4.2.7.2.2-((1-(2-cyclopropylacetyl)piperidin-4-yl)amino)-5-(hex-1-yn-1-yl)benzamide (28). Compound **28** was prepared from **24** (150 mg, 0.5 mmol) and 2-cyclopropylacetic acid (100 mg, 1.0 mmol) according to the general procedures. White solid (133 mg, 69.8%). Mp 133.4–135.3 °C. <sup>1</sup>H NMR (300 MHz, DMSO-*d*<sub>6</sub>) δ 8.41 (d, *J* = 7.7 Hz, 1H), 7.92 (s, 1H), 7.65 (s, 1H), 7.23 (d, *J* = 8.1 Hz, 1H), 7.18 (s, 1H), 6.72 (d, *J* = 8.9 Hz, 1H), 4.14–4.10 (m, 1H), 3.74–3.70 (m, 1H), 3.64–3.57 (m, 1H), 3.19 (t, *J* = 12.1 Hz, 1H), 2.89 (t, *J* = 11.7 Hz, 1H), 2.35 (t, *J* = 6.7 Hz, 2H), 2.24 (d, *J* = 6.8 Hz, 2H), 1.96–1.86 (m, 2H), 1.48–1.37 (m, 4H), 1.28–1.21 (m, 3H), 0.89 (t, *J* = 6.9 Hz, 3H), 0.42 (d, *J* = 7.7 Hz, 2H), 0.09 (d, *J* = 4.1 Hz, 2H). HRMS (ESI): calcd for C<sub>23</sub>H<sub>31</sub>N<sub>3</sub>O<sub>2</sub> [M + Na]<sup>+</sup> 404.24, found 404.23. Purity: 96.39% by HPLC (MeOH/H<sub>2</sub>O = 90:10). R<sub>f</sub>: 0.25 by TLC (PE/EA = 1:1).

4.2.7.3.2-((1-(dimethylglycyl)piperidin-4-yl)amino)-5-(hex-1-yn-1-yl)benzamide (29). Compound **29** was prepared from **24** (150 mg, 0.5 mmol) and dimethylglycine (103.1 mg, 1.0 mmol) according to the general procedures. White solid (65 mg, 33.8%). Mp 153.9–155.6 °C. <sup>1</sup>H NMR (300 MHz, DMSO-*d*<sub>6</sub>) δ 8.43 (d, *J* = 7.6 Hz, 1H), 7.93 (s, 1H), 7.67 (s, 1H), 7.25 (d, *J* = 8.9 Hz, 1H), 7.19 (s, 1H), 6.74 (d, *J* = 8.8 Hz, 1H), 4.13–4.08 (m, 1H), 3.93–3.89 (m, 1H), 3.66–3.60 (m, 1H), 3.22–3.03 (m, 3H), 2.95–2.87 (m, 1H), 2.54 (s, 3H), 2.37 (t, *J* = 6.5 Hz, 2H), 2.19 (s, 3H), 1.96–1.92 (m, 2H), 1.55–1.39 (m, 4H), 1.24–1.16 (m, 2H), 0.91 (t, *J* = 6.9 Hz, 3H). HRMS (ESI): calcd for C<sub>22</sub>H<sub>32</sub>N<sub>4</sub>O<sub>2</sub> [M + H]<sup>+</sup> 385.25, found 385.26. Purity: 97.73% by HPLC (MeOH/H<sub>2</sub>O = 90:10). R<sub>f</sub>: 0.4 by TLC (PE/EA = 2:1).

4.2.7.4.2-((1-(2-morpholinoacetyl)piperidin-4-yl)amino)-5-

(hex-1-yn-1-yl)benzamide (**30**). Compound **30** was prepared from **24** (150 mg, 0.5 mmol) and 2-morpholinoacetic acid (145.1 mg, 1.0 mmol) according to the general procedures. White solid (137 mg, 64.3%). Mp 91.2–92.7 °C. <sup>1</sup>H NMR (300 MHz, DMSO-*d*<sub>6</sub>) δ 8.43 (d, *J* = 7.6 Hz, 1H), 7.93 (s, 1H), 7.68 (s, 1H), 7.26 (d, *J* = 8.6 Hz, 1H), 7.17 (s, 1H), 6.74 (d, *J* = 8.8 Hz, 1H), 4.12–4.07 (m, 1H), 3.95–3.91 (m, 1H), 3.72–3.61 (m, 1H), 3.61–3.53 (m, 4H), 3.25–3.20 (m, 2H), 3.11–3.06 (m, 1H), 2.97–2.89 (m, 1H), 2.42–2.36 (m, 6H), 1.99–1.91 (m, 2H), 1.54–1.39 (m, 4H), 1.28–1.19 (m, 2H), 0.91 (t, *J* = 7.1 Hz, 3H). HRMS (ESI): calcd for C<sub>24</sub>H<sub>34</sub>N<sub>4</sub>O<sub>3</sub> [M + H]<sup>+</sup> 427.26, found 427.27. Purity: 99.35% by HPLC (MeOH/H<sub>2</sub>O = 90:10). R<sub>f</sub>: 0.3 by TLC (DCM/MeOH = 20:1).

4.2.7.5.2-((1-(3-morpholinopropanoyl)piperidin-4-yl)amino)-5-(hex-1-yn-1-yl)benzamide (**31**). Compound **31** was prepared from **24** (120 mg, 0.4 mmol) and 3-morpholinopropanoic acid (127.3 mg, 0.8 mmol) according to the general procedures. Light yellow solid (102 mg, 57.9%). Mp 65.5–66.9 °C. <sup>1</sup>H NMR (300 MHz, DMSO-*d*<sub>6</sub>) δ 8.44 (d, *J* = 7.7 Hz, 1H), 7.93 (s, 1H), 7.68 (s, 1H), 7.26 (d, *J* = 8.7 Hz, 1H), 7.17 (s, 1H), 6.75 (d, *J* = 8.8 Hz, 1H), 4.16–4.11 (m, 1H), 3.80–3.66 (m, 6H), 3.25–3.20 (m, 2H), 2.99–2.91 (m, 2H), 2.73–2.60 (m, 4H), 2.38 (t, *J* = 6.6 Hz, 2H), 1.99–1.92 (m, 2H), 1.53–1.34 (m, 4H), 1.25–1.23 (m, 2H), 0.92 (t, *J* = 7.0 Hz, 3H). HRMS (ESI): calcd for C<sub>25</sub>H<sub>36</sub>N<sub>4</sub>O<sub>3</sub> [M + H]<sup>+</sup> 441.28, found 441.29. Purity: 99.34% by HPLC (MeOH/H<sub>2</sub>O = 90:10). R<sub>f</sub>: 0.2 by TLC (DCM/MeOH = 20:1).

4.2.7.6.2-(((1-acetylpiperidin-4-yl)methyl)amino)-5-(hex-1-yn-1-yl)benzamide (**32**). Compound **32** was prepared from **25** (156.6 mg, 0.5 mmol) and acetic acid (60 mg, 1.0 mmol) according to the general procedures. Light yellow solid (102 mg, 57.9%). White solid (87 mg, 45.6%). Mp 137.9–140.4 °C. <sup>1</sup>H NMR (300 MHz, DMSO-*d*<sub>6</sub>) δ 8.52–8.38 (m, 1H), 7.92 (s, 1H), 7.66 (s, 1H), 7.24 (d, *J* = 9.6 Hz, 1H), 7.17 (s, 1H), 6.64 (d, *J* = 8.9 Hz, 1H), 4.37 (d, *J* = 12.3 Hz, 1H), 3.81 (d, *J* = 14.6 Hz, 1H), 3.07–2.88 (m, 3H), 2.43 (d, *J* = 5.8 Hz, 1H), 2.37 (t, *J* = 6.6 Hz, 2H), 1.97 (s, 3H), 1.83–1.63 (m, 3H), 1.45 (dq, *J* = 20.2, 7.3, 6.5 Hz, 4H), 1.23 (s, 2H), 0.90 (t, *J* = 7.0 Hz, 3H). HRMS (ESI): calcd for C<sub>23</sub>H<sub>31</sub>N<sub>3</sub>O<sub>2</sub> [M + Na]<sup>+</sup> 378.23, found 378.22. Purity: 97.57% by HPLC (MeOH/H<sub>2</sub>O = 90:10). R<sub>f</sub>: 0.4 by TLC (DCM/MeOH = 20:1).

4.2.7.7.2-(((1-(cyclopropanecarbonyl)piperidin-4-yl)methyl)amino)-5-(hex-1-yn-1-yl)benzamide (**33**). Compound **33** was prepared from **25** (156.6 mg, 0.5 mmol) and cyclopropanecarboxylic acid (86 mg, 1.0 mmol) according to the general procedures. White solid (126 mg, 70.9%). Mp 145.6–146.8 °C. <sup>1</sup>H NMR (300 MHz, DMSO-*d*<sub>6</sub>) δ 8.54–8.42 (m, 1H), 7.95 (s, 1H), 7.67 (s, 1H), 7.25 (d, *J* = 8.5 Hz, 1H), 7.19 (s, 1H), 6.65 (d, *J* = 8.1 Hz, 1H), 4.43–4.22 (m, 2H), 3.15–2.92 (m, 3H), 2.58 (s, 1H), 2.43–2.31 (m, 2H), 2.02–1.91 (m, 1H), 1.86–1.63 (m, 3H), 1.58–1.37 (m, 4H), 1.30–1.21 (m, 2H), 0.91 (t, *J* = 7.1 Hz, 3H), 0.67 (d, *J* = 7.9 Hz, 4H). HRMS (ESI): calcd for C<sub>21</sub>H<sub>29</sub>N<sub>3</sub>O<sub>2</sub> [M + Na]<sup>+</sup> 404.24, found 404.23. Purity: 97.57% by HPLC (MeOH/H<sub>2</sub>O = 90:10). R<sub>f</sub>: 0.25 by TLC (PE/Ea = 1:1).

4.2.7.8.2-((1-acetylpiperidin-3-yl)amino)-5-(hex-1-yn-1-yl)benzamide (**34**). Compound **34** was prepared from **26** (120 mg, 0.4 mmol) and acetic acid (48 mg, 0.8 mmol) according to the general procedures. White solid (112 mg, 82.1%). Mp 97.4–99.0 °C. <sup>1</sup>H NMR (300 MHz, chloroform-*d*) δ 8.14 (dd, *J* = 45.6, 7.1 Hz, 1H), 7.49 (d, *J* = 11.3 Hz, 1H), 7.41–7.33 (m, 1H), 6.73 (dd, *J* = 46.3, 8.6 Hz, 1H), 5.75 (s, 2H), 4.27 (dd, *J* = 196.6, 12.8 Hz, 1H), 3.75 (dd, *J* = 27.3, 12.8 Hz, 1H), 3.50 (d, *J* = 33.8 Hz, 1H), 3.32–3.14 (m, 1H), 2.79–2.66 (m, 1H), 2.42 (t, *J* = 6.4 Hz, 2H), 2.12 (d, *J* = 24.8 Hz, 4H), 1.96–1.80 (m, 1H), 1.66–1.50 (m, 6H), 0.98 (t, *J* = 7.0 Hz, 3H). HRMS (ESI): calcd for C<sub>20</sub>H<sub>27</sub>N<sub>3</sub>O<sub>2</sub> [M + Na]<sup>+</sup> 364.21, found 364.20. Purity: 99.34% by HPLC (MeOH/H<sub>2</sub>O = 90:10). R<sub>f</sub>: 0.5 by TLC (DCM/MeOH = 20:1).

## 5. Biology

### 5.1. Protein expression and purification

Canine Grp94<sup>NΔ41</sup> (residues 69–337; residues 286–328 from the charged linker were replaced by four glycine residues) was overexpressed in *E. coli* strain BL21 star (DE3) as GST fusions. The purification was in accordance with the protocol using GSTrap HP column (GE Healthcare, Sweden, 17528202). The N-terminal domain of human Hsp90α (residues 1–236) was also expressed in *E. coli* strain BL21 star (DE3) as His fusions. The purification of His-tagged Hsp90α<sup>N</sup> was as described using HisTrap HP column (GE Healthcare, Sweden, 17528202).

### 5.2. Fluorescent polarization assay

All fluorescent polarization (FP) experiments were performed on the SpectraMax multimode microplate reader (Molecular Devices) with excitation and emission wavelength at 485 and 535 nm, respectively. The assay was performed in 384-well format in black, flat bottom plates (Corning no. 3575) with a final volume of 60 μL. 20 μL of assay buffer (20 mM HEPES, 50 mM KCl, 5 mM MgCl<sub>2</sub>, pH 7.4, 2 mM DTT, 0.1 mg/ml BGG, and 0.01% NP-40) containing three-fold serial dilutions of compounds (the starting and final concentrations were 60 μM and 0.33 nM, respectively), 20 μL of assay buffer containing 60 nM of either purified Grp94<sup>N</sup> or Hsp90α<sup>N</sup>, and 20 μL of assay buffer containing 18 nM GM-FITC (fluorescent tracer, stock in DMSO and diluted in assay buffer) were added to each well. For each assay, negative controls (GM-FITC only), positive controls (GM-FITC in the presence of Grp94<sup>N</sup> or Hsp90α<sup>N</sup>), and test wells (inhibitors and GM-FITC in the presence of Grp94<sup>N</sup> or Hsp90α<sup>N</sup>) were included on each assay plate. Plates were incubated with rocking for 4 h at 4 °C in the dark. IC<sub>50</sub> values were calculated using GraphPad Prism 6.0 software.

### 5.3. BLI assay

As a mature biophysical assay, we chose biolayer interferometry (BLI) as another method to revalidate candidates identified as inhibitors by the FP competition assay. Biolayer interferometry assays on Octet Red 96 instrument (FortéBio, MenloPark, CA, USA) were used to determine the interaction between the ligand and protein. Proteins used in this assay were all biotinylated by EZ-link sulfo-NHS-LC-biotinylation kit (no. 21340, Thermo Pierce) in 1 × PBS (pH 7.4). Super Streptavidin (SSA) biosensors tips (FortéBio, Inc., Menlo Park, CA) were prewetted by dipping them into kinetics buffer (PBS, 0.05% BSA, 0.01% Tween-20) for 10 min before use, and they were incubated with biotinylated Grp94<sup>N</sup> (a final concentration of 400 nM) or Hsp90α<sup>N</sup> (a final concentration of 400 nM) to immobilize the protein on sensor tips. Different concentrations of compound **4** were added to be immobilized onto SSA sensors. All the data were collected at 30 °C and analyzed on Octet data analysis software (7.1). The signals were corrected each step and analyzed using a double reference subtraction protocol to fit globally to a 1:1 binding model. The equilibrium dissociation constant (K<sub>D</sub>) values were calculated from the ratio of K<sub>off</sub> to K<sub>on</sub> (K<sub>D</sub> = K<sub>off</sub>/K<sub>on</sub>).

### 5.4. Microsomal stability assay

10 μM compound **4** or **DDO-5813** was preincubated with MgCl<sub>2</sub> (10 mM), human microsomes (0.2 mg/ml) or mouse microsomes (0.5 mg/ml) for 5 min at 37 °C in phosphate buffer (100 mM, pH = 7.4). The addition of 1 mM NADPH initiated the reactions. After 0, 5, 10, 30, 60, 90, 120 min incubations at 37 °C, the cold acetonitrile with an internal standard (Reserpine, 10 ng/ml) was

utilized to precipitate the protein. Lastly, the supernatants were used for analysis using a developed LC-MS/MS method.

### 5.5. Pharmacokinetic experiments

All animal care and in vivo procedures conducted were in accordance with the guidelines of Institutional Animal Care and Use Committee of China Pharmaceutical University. Compound **4** was tested in pharmacokinetic studies on Sprague Dawley® (SD) rats weighing 220–240 g, with six rats (male) in each group. Animals were allowed ad libitum access to water and food. The test compound was administered orally (po) at a dose of 40 mg/kg or intravenously (iv) at a dose of 10 mg/kg. After dosing, serial blood samples were collected via the retrobulbar vein at indicated time points (0, 0.167, 0.25, 0.5, 1, 2, 4, 8, 12, and 24 h). Blood samples in heparinized Eppendorf tubes were centrifuged at 3000 rpm for 10 min to get plasma samples, which were stored at –20 °C until analysis by LC-MS/MS. The PK parameters were then calculated using a non-atrioventricular model (Phoenix WinNonlin 7.0, Pharsight).

### 5.6. Induction of UC model and compound 4 treatment

Male C57BL/6 mice (20–22 g) were purchased from Jinan Pengyue Laboratory Animal Breeding Co. Ltd. and randomly divided into five groups (n = 8 per group): normal control group, disease control group, compound **4** group (10 mg/kg), compound **4** group (30 mg/kg), compound **4** group (50 mg/kg). The studies were conducted in accordance with the guidelines of Institutional Animal Care and Use Committee of China Pharmaceutical University. The normal control group mice were given distilled water, and the other four groups were given 3% DSS (36–50 KD) orally in drinking water to induce UC for 7 days. All animals had free access to food and water, which were changed every day. The compound **4**-treated groups were co-administrated (ip, q.d.) with DSS, while normal control group and disease control group mice were treated with vehicle. The changes in body weight, stool consistency, and rectal bleeding of all mice were recorded once a day. The colons were collected and measured when experimental mice were sacrificed on day 8. The serum was used for the determination of cytokines. Sections of distal colons were excised, fixed in 4% formaldehyde, and preserved for H&E staining analysis. The remaining parts of the colons were immediately flash-frozen in liquid nitrogen for further examination.

### 5.7. Calculation of disease activity index (DAI) scores

DAI scores were calculated daily according to general clinical symptoms, including body weight loss, stool consistency, and stool blood. The mean of the scores of the three symptoms was calculated as DAI score.

### 5.8. Hematoxylin-eosin (H&E) staining

Colon tissues were fixed in 4% formaldehyde solution, and embedded in paraffin. Then, they were cut to make the thickness 5 µm and stained with H&E. The sections were detected under an optical microscope (Olympus CKX53, Tokyo, Japan).

### 5.9. Enzyme-linked immunosorbent assay (ELISA)

The mouse colon tissues were fully ground and centrifuged at 3000 rpm for 15 min to afford the supernatants. A standard ELISA assay was performed according to the protocol recommended by the manufacturer. ELISA kits were used to measure the expression

levels of inflammatory cytokines (IL-6 and TNF-α). Mouse IL-6 ELISA kit (Catalog #EK0411) and TNF-α ELISA kit (Catalog #EK0527) were provided by Boster Biological Technology Co. Ltd. Plates were read in a SpectraMax Plus microplate reader (Molecular Devices) at 492 nm.

### 5.10. Immunohistochemistry

Colon samples, fixed in 4% formalin, were embedded in paraffin and cut into 5 µm sections. Then the paraffin sections were deparaffinized through a graded alcohol series to water and PBS. The sections were incubated in 3% hydrogen peroxide (H<sub>2</sub>O<sub>2</sub>) to quench the endogenous peroxidase. All the slides were incubated with the primary antibody overnight at 4 °C after they were blocked with 10% normal goat serum in 2% PBS. Then, the secondary antibody was incubated with the slides at 37 °C for 20 min. DAB and hematoxylin were used to stain and retain the samples, respectively. A light microscope (200 ×, Nikon, Tokyo, Japan) coupled with a charge-coupled device camera was used to obtain all photomicrographs.

## 6. Docking

The complex structure of PU-H54 and Grp94<sup>N</sup> (PDB ID: 3O2F) was obtained from the Protein Data Bank (PDB). All compounds and the protein structures needed for docking were prepared by Discovery Studio (DS) 4.0 software. The water molecules HOH22, HOH441, which are conserved in the binding site, are kept for docking. The conformations of protein and compounds were generated with the protocol “Prepare Protein” and “Prepare Ligands”, respectively. The residues of Grp94 around compound **4** (radius 11.0 Å) were defined as the binding site, which completely covered the binding site. The molecular docking using the “CDOCKER” tool was performed, and other docking processes were default.

### Declaration of competing interest

The authors declare that they have no known competing financial interests or personal relationships that could have appeared to influence the work reported in this paper.

### Acknowledgments

This work was supported by Projects 82073766, 81872737, and 81930100 of the National Natural Science Foundation of China; BK20201331 of Foundation Research Project of Jiangsu Province; [GrantCPU2018GY02] of Double First Class Innovation Team of China Pharmaceutical University; the Project Program of State Key Laboratory of Natural Medicines, China Pharmaceutical University (No. SKLNMZZ202003); the Priority Academic Program Development of Jiangsu Higher Education Institutions; Qinglan Project of Jiangsu Province.

### Appendix A. Supplementary data

Supplementary data to this article can be found online at <https://doi.org/10.1016/j.ejmech.2021.113604>.

### References

- [1] L. Whitesell, S.L. Lindquist, HSP90 and the chaperoning of cancer, *Nat. Rev. Canc.* 5 (2005) 761–772.
- [2] C.K. Vaughan, L. Neckers, P.W. Piper, Understanding of the Hsp90 molecular chaperone reaches new heights, *Nat. Struct. Mol. Biol.* 17 (2010) 1400–1404.
- [3] K. Richter, L.M. Hendershot, B.C. Freeman, The cellular world according to

- Hsp90, *Nat. Struct. Mol. Biol.* 14 (2007) 90–94.
- [4] Y. Miyata, H. Nakamoto, L. Neckers, The therapeutic target Hsp90 and cancer hallmarks, *Curr. Pharmaceut. Des.* 19 (2013) 347–365.
- [5] F.U. Hartl, A. Bracher, M. Hayer-Hartl, Molecular chaperones in protein folding and proteostasis, *Nature*. 475 (2011) 324–332.
- [6] R. Bhat, S.R. Tummalappalli, D.P. Rotella, Progress in the discovery and development of heat shock protein 90 (Hsp90) inhibitors, *J. Med. Chem.* 57 (2014) 8718–8728.
- [7] M.A. Biamonte, et al., Heat shock protein 90: inhibitors in clinical trials, *J. Med. Chem.* 53 (2010) 3–17.
- [8] L. Neckers, P. Workman, Hsp90 molecular chaperone inhibitors: are we there yet? *Clin. Canc. Res.* 18 (2012) 64–76.
- [9] J. Koren III, B.S.J. Blagg, The right tool for the job: an overview of Hsp90 inhibitors, *Adv. Exp. Med. Biol.* 1243 (2020) 135–146.
- [10] S.J. Mishra, et al., The development of Hsp90 $\beta$ -selective inhibitors to overcome detriments associated with pan-Hsp90 inhibition, *J. Med. Chem.* 64 (2021) 1545–1557.
- [11] R. Bagatell, et al., Induction of a heat shock factor 1-dependent stress response alters the cytotoxic activity of Hsp90-binding agents, *Clin. Canc. Res.* 6 (2000) 3312–3318.
- [12] A. Khandelwal, V.M. Crowley, B.S.J. Blagg, Natural product inspired N-terminal Hsp90 inhibitors: from bench to bedside? *Med. Res. Rev.* 36 (2016) 92–118.
- [13] V.C. Birar, I. Gelis, A. Zuo, B.S.J. Blagg, Synthesis of paramagnetic ligands that target the C-terminal binding site of Hsp90, *Bioorg. Med. Chem. Lett.* 30 (2020) 127303.
- [14] K.W. Pugh, et al., From bacteria to cancer: a benzothiazole-based DNA gyrase B inhibitor redesigned for Hsp90 C-terminal inhibition, *ACS Med. Chem. Lett.* 11 (2020) 1535–1538.
- [15] X.M. Yu, et al., Hsp90 inhibitors identified from a library of novobiocin analogues, *J. Am. Chem. Soc.* 127 (2005) 12778–12779.
- [16] D.-J. Chang, et al., Design, synthesis, and biological evaluation of novel deguelin-based heat shock protein 90 (HSP90) inhibitors targeting proliferation and angiogenesis, *J. Med. Chem.* 55 (2012) 10863–10884.
- [17] L. Wang, et al., Discovery and optimization of small molecules targeting the protein-protein interaction of heat shock protein 90 (Hsp90) and cell division cycle 37 as orally active inhibitors for the treatment of colorectal cancer, *J. Med. Chem.* 63 (2020) 1281–1297.
- [18] X. Chen, et al., DCZ3112, a novel Hsp90 inhibitor, exerts potent antitumor activity against HER2-positive breast cancer through disruption of Hsp90-Cdc37 interaction, *Canc. Lett.* 434 (2018) 70–80.
- [19] S.C. Stiegler, et al., A chemical compound inhibiting the Aha1-Hsp90 chaperone complex, *J. Biol. Chem.* 292 (2017) 17073–17083.
- [20] A. Chadli, et al., Celestrol inhibits Hsp90 chaperoning of steroid receptors by inducing fibrillization of the Co-chaperone p23, *J. Biol. Chem.* 285 (2010) 4224–4231.
- [21] S.J. Mishra, et al., Selective inhibition of the Hsp90 $\alpha$  isoform, *Angew. Chem. Int. Ed.* 60 (2021) 10547–10551.
- [22] A. Khandelwal, et al., Structure-guided design of an Hsp90 $\beta$  N-terminal isoform-selective inhibitor, *Nat. Commun.* 9 (2018) 425.
- [23] P.D. Patel, et al., Paralog-selective Hsp90 inhibitors define tumor-specific regulation of HER2, *Nat. Chem. Biol.* 9 (2013) 677–684.
- [24] C. Lee, et al., Development of a mitochondria-targeted Hsp90 inhibitor based on the crystal structures of human TRAP1, *J. Am. Chem. Soc.* 137 (2015) 4358–4367.
- [25] H.-K. Park, et al., Paralog specificity determines subcellular distribution, action mechanism, and anticancer activity of TRAP1 inhibitors, *J. Med. Chem.* 60 (2017) 7569–7578.
- [26] G. Chiosis, C.A. Dickey, J.L. Johnson, A global view of Hsp90 functions, *Nat. Struct. Mol. Biol.* 20 (2013) 1–4.
- [27] D.T. Gewirth, Paralog specific Hsp90 inhibitors - a brief history and a bright future, *Curr. Top. Med. Chem.* 16 (2016) 2779–2791.
- [28] B. Liu, et al., Cell surface expression of an endoplasmic reticulum resident heat shock protein gp96 triggers MyD88-dependent systemic autoimmune diseases, *Proc. Natl. Acad. Sci. U.S.A.* 100 (2003) 15824–15829.
- [29] E.A. Ansa-Addo, et al., Clients and oncogenic roles of molecular chaperone gp96/grp94, *Curr. Top. Med. Chem.* 16 (2016) 2765–2778.
- [30] O. Ostrovsky, N.T. Ahmed, Y. Argon, The chaperone activity of GRP94 toward insulin-like growth factor II is necessary for the stress response to serum deprivation, *Mol. Biol. Cell.* 20 (2009) 1855–1864.
- [31] D.E. Dollins, R.M. Immormino, D.T. Gewirth, Structure of unliganded GRP94, the endoplasmic reticulum Hsp90: basis for nucleotide-induced conformational change, *J. Biol. Chem.* 280 (2005) 30438–30447.
- [32] K.L. Soldano, A. Jivan, C.V. Nicchitta, D.T. Gewirth, Structure of the N-terminal domain of GRP94: basis for ligand specificity and regulation, *J. Biol. Chem.* 278 (2003) 48330–48338.
- [33] D.E. Dollins, J.J. Warren, R.M. Immormino, D.T. Gewirth, Structures of GRP94-nucleotide complexes reveal mechanistic differences between the hsp90 chaperones, *Mol. Cell.* 28 (2007) 41–56.
- [34] K.A. Maharaj, et al., Exploring the functional complementation between Grp94 and Hsp90, *PLoS One.* 11 (2016) e0166271.
- [35] A.S. Duerfeldt, et al., Development of a Grp94 inhibitor, *J. Am. Chem. Soc.* 134 (2012) 9796–9804.
- [36] N.L.S. Que, et al., Structure based design of a Grp94-selective inhibitor: exploiting a key residue in Grp94 to optimize paralog-selective binding, *J. Med. Chem.* 61 (2018) 2793–2805.
- [37] T. Taldone, et al., Experimental and structural testing module to analyze paralog-specificity and affinity in the Hsp90 inhibitors series, *J. Med. Chem.* 56 (2013) 6803–6818.
- [38] R.M. Immormino, et al., Different poses for ligand and chaperone in inhibitor-bound Hsp90 and GRP94: implications for paralog-specific drug design, *J. Mol. Biol.* 388 (2009) 1033–1042.
- [39] J.J. Wassenberg, R.C. Reed, C.V. Nicchitta, Ligand interactions in the adenosine nucleotide-binding domain of the Hsp90 chaperone, GRP94. II. Ligand-mediated activation of GRP94 molecular chaperone and peptide binding activity, *J. Biol. Chem.* 275 (2000) 22806–22814.
- [40] D.K. Tosh, et al., Biological evaluation of 5'-(N-Ethylcarboxamido)adenosine analogues as Grp94-selective inhibitors, *ACS Med. Chem. Lett.* 12 (2021) 373–379.
- [41] V.M. Crowley, et al., Development of glucose regulated protein 94-selective inhibitors based on the Bnlm and Radamide scaffold, *J. Med. Chem.* 59 (2016) 3471–3488.
- [42] A. Khandelwal, V.M. Crowley, B.S.J. Blagg, Resorcinol-based Grp94-selective inhibitors, *ACS Med. Chem. Lett.* 8 (2017) 1013–1018.
- [43] F. Jiang, A.-p. Guo, J.-c. Xu, Q.-D. You, X.-L. Xu, Discovery of a potent Grp94 selective inhibitor with anti-inflammatory efficacy in a mouse model of ulcerative colitis, *J. Med. Chem.* 61 (2018) 9513–9533.
- [44] T. Apelqvist, D. Wensbo, Selective removal of the N-BOC protective group using silica gel at low pressure, *Tetrahedron Lett.* 37 (1996) 1471–1472.
- [45] A.M. Jarrad, et al., Nitroimidazole carboxamides as antiparasitic agents targeting *Giardia lamblia*, *Entamoeba histolytica* and *Trichomonas vaginalis*, *Eur. J. Med. Chem.* 120 (2016) 353–362.
- [46] R.J. Xavier, D.K. Podolsky, Unravelling the pathogenesis of inflammatory bowel disease, *Nature*. 448 (2007) 427–434.
- [47] B. Liu, et al., Essential roles of grp94 in gut homeostasis via chaperoning canonical Wnt pathway, *Proc. Natl. Acad. Sci. U.S.A.* 110 (2013) 6877–6882.
- [48] Y. Hua, et al., Gut homeostasis and regulatory T cell induction depend on molecular chaperone gp96 in CD11c+ cells, *Sci. Rep.* 7 (2017) 1–14.
- [49] K. Schreitner, et al., Glycoprotein (gp) 96 expression: induced during differentiation of intestinal macrophages but impaired in Crohn's disease, *Gut.* 54 (2005) 935–943.